sustainability

MDPI

Article

Analysis of Key Factors for Natural Regeneration of Cypress Forests in the Karst Area of the Lijiang River

Yu Gan [1,2], Dingyuan Liu [3], Ying Huang [4], Haitao Yu [4] and Weiqun Luo [1,*]

[1] Key Laboratory of Karst Ecosystem and Treatment of Rocky Desertification, Ministry of Natural Resources, Institute of Karst Geology, Guilin 541004, China; 2016210003@gxufe.edu.cn
[2] School of Finance and Insurance, Guangxi University of Finance and Economics, Nanning 530007, China
[3] Shandong Lan'an Landscape Engineering Co., Ltd., Jinan 250013, China
[4] Department of Tourism and Landscape Architecture, Guilin University of Technology, Guilin 541004, China
* Correspondence: lweiqun@mail.cgs.gov.cn; Tel.: +86-1857-796-1034

Abstract

The natural regeneration of planted forests in karst landscapes is severely constrained by extreme substrate heterogeneity and fragile edaphic conditions. However, the relative importance and interaction pathways of environmental versus stand structural drivers remain poorly quantified. In this study, 54 plots (10 m × 10 m) were surveyed across *Cupressus funebris* plantations in the karst landscape of the Lijiang River Basin, southern China. To identify the key factors and causal pathways governing regeneration, redundancy analysis (RDA), variation partitioning, partial least squares structural equation modeling (PLS-SEM), and threshold analyses were applied. Regeneration exhibited pronounced spatial heterogeneity, with 42.6% of plots showing complete recruitment failure and a characteristic inverted J-shaped size class distribution. The analysis identified soil rock fragment content (as a negative constraint) and canopy gap area (as a positive driver) as the two dominant predictors. PLS-SEM revealed that environmental factors influence regeneration primarily through an indirect pathway mediated by stand structure ($R^2 = 0.683$) rather than through direct effects. Threshold analyses identified quantitative benchmarks for key drivers, including a gap area breakpoint of approximately 10 m^2 and a presence–absence effect of soil rock fragments. These findings contribute to a more sophisticated mechanistic understanding of forest regeneration in karst ecosystems and provide an empirical foundation for silvicultural management that aims to encourage natural regeneration and ecological restoration of degraded karst plantations.

Keywords: *Cupressus funebris*; natural regeneration; karst vegetation; environmental 20 factors; stand structure; ecological restoration

Check for updates

Academic Editor: Lucian Dinca

Received: 29 January 2026
Revised: 27 February 2026
Accepted: 11 March 2026
Published: 15 March 2026

Copyright: © 2026 by the authors. Licensee MDPI, Basel, Switzerland. This article is an open access article distributed under the terms and conditions of the Creative Commons Attribution (CC BY) license.

1. Introduction

Natural forest regeneration is a complex biological process that operates independently of anthropogenic control, relying fundamentally on the intrinsic reproductive capacity of forest ecosystems to establish new cohorts [1]. This autonomous renewal process is critical for ensuring the sustainable survival and reproduction of populations, maintaining the stability of community composition and structure, and holding significant implications for vegetation restoration and community succession [2]. However, ecosystem services essential for supporting all life on Earth are currently being compromised by extensive forest transformation. Specifically, the redirection of over 50% of tropical forests to alternative land uses has resulted in a marked decline in critical habitats and available resources [3,4].

In recent years, a growing body of research has demonstrated that natural regeneration is modulated by a diverse array of drivers, including tree species functional traits, stand characteristics, edaphic conditions, environmental heterogeneity, disturbance regimes, and faunal interactions [5–7].

Among these drivers, environmental and stand factors—such as slope aspect, altitude, forest gaps, canopy closure, and shrub-herb coverage—have received extensive scholarly attention. For instance, Lu et al. (2019) investigated natural forests of *Quercus aliena* var. *acutiserrata* across different slope aspects in the middle Qinling Mountains, discovering that semi-sunny slopes are significantly more conducive to seed germination and regeneration establishment [8]. Regarding elevational gradients, Redmond and Kelsey (2018) observed a strong negative correlation between the density of young Engelmann spruce and altitude, noting that these populations remained relatively resilient to estimated warming temperatures [9]. In terms of gap dynamics, Zhang et al. (2022) studied the natural regeneration status of *Larix gmelinii* var. *principis-rupprechtii* plantations in Mount Guandi, concluding that regeneration density and growth indicators are significantly positively impacted by increasing gap area [10]. Similarly, regarding canopy influence, Wang et al. (2020) conducted a study on the regeneration of *Pinus koraiensis*, *Picea koraiensis*, and *Fraxinus mandshurica* within *Larix olgensis* plantations, finding that the height growth of all three species exhibited an increasing trend with decreasing canopy density [11]. Furthermore, biotic competition plays a crucial role; Huong et al. (2016) examined the impact of understory structure on the regeneration of *Scaphium wallichii* and noted that increased shrub and herb coverage, combined with lower shrub height, created conditions unfavorable for the regeneration of young tree seedlings [12].

Currently, research on natural forest regeneration remains predominantly focused on temperate and tropical humid regions (e.g., Northeastern China and the Amazon rainforests), where natural regeneration is relatively easier to achieve due to mild climates, higher soil fertility, and a lower frequency of disturbances [13]. For example, the regeneration potential of beech forests in Europe and East Asia has been well-verified through numerous empirical experiments [14]. Nevertheless, karst landscapes are generally regarded as recalcitrant sites for forest regeneration due to their unique and harsh geological conditions, such as intense karstification, nutrient-poor soils, and poor water retention capacity. Simultaneously, at the species level, most existing studies have focused on fast-growing taxa or drought-tolerant species, which have historically been the mainstream selection for plantation forestry due to their adaptability and high reproductive efficiency [15]. However, the specific ecological constraints of karst regions—such as carbonate substrates and extreme soil erosion—often make it difficult for these conventional species to survive, underscoring an urgent necessity to screen for native species possessing specific adaptations to these environments.

Relatively, there is a paucity of research regarding the natural regeneration of forests specifically within the karst area of the Lijiang River Basin. The terrain and topography of this region are unique, characterized by abundant and concentrated rainfall and thermal resources, yet paradoxically constrained by strong carbonate rock dissolution, poor soil fertility, low vegetation coverage, high permeability, and poor water-holding capacity [16]. These factors contribute to a fragile habitat with low ecosystem stability and weak resistance to interference, making the system highly susceptible to degradation under human disturbance and rendering recovery exceptionally difficult [17]. *Cupressus funebris* (cypress) is an evergreen tree species in the Cupressaceae family that is well-adapted to these challenging conditions. It prefers warm and humid climates and demonstrates strong adaptability to neutral, slightly acidic, and calcareous soils, particularly the shallow calcareous purple soils and upper calcareous soils typical of the region [18–20]. As a result, it is considered an

important tree species for afforestation in karst barren mountains. Therefore, to prevent further rocky desertification, cypress is frequently selected as the pioneer species for establishing artificial forests on rocky slopes, aiming to optimize tree species structure and improve overall forest quality [21,22].

However, restoring cypress forests through natural regeneration poses significant challenges and considerably reduces the efficiency of regional ecological restoration efforts [23–25]. Given that cypress acts as the main dominant species in the Lijiang karst area of Guilin [26], studying the factors influencing the natural regeneration of artificial karst cypress forests is essential for maintaining community stability and promoting forest succession. Such research provides an important theoretical and practical basis for ecological vegetation reconstruction and biological resource protection in areas subject to human interference. Consequently, this article takes the artificial cypress forest in the karst area of the Lijiang River Basin as the research object to investigate the characteristics of cypress regeneration and the environmental and stand factors that may affect this process. It attempts to elucidate the impact of these biotic and abiotic factors on cypress regeneration, providing a reference basis for future research on regeneration mechanisms and the management of artificial cypress forests, while fostering discussions beneficial for ecological protection and restoration work in the Lijiang River karst area.

2. Materials and Methods

2.1. Study Area

This comprehensive investigation was conducted within the typical karst landform regions of the Lijiang River Basin, geographically spanning from Guilin city to Yangshuo County (24°56′–25°17′ N, 110°17′–110°29′ E), China (Figure 1) [27]. The region is characterized by a subtropical monsoon climate, endowed with abundant precipitation and sufficient solar radiation, creating a unique hydrothermal environment. Climatological data indicates that the mean annual temperature is approximately 19.2 °C. The region exhibits distinct seasonal thermal variations: July and August represent the warmest period of the year, with an average temperature of approximately 28.5 °C, whereas January and February constitute the coldest period, with an average temperature of approximately 8.3 °C. The hydrological regime is robust, with an annual average rainfall of 1949.5 mm, and the relative humidity remains consistently high, ranging from 73% to 79% annually. Solar resources are significant, with an annual average sunshine duration of 1670 h, and the average atmospheric pressure is recorded at 994.9 hPa [28].

The specific survey sites selected for this study are situated within *Cupressus funebris* (cypress) forests. These forests are of particular historical and ecological significance, as *Cupressus funebris* has served as the primary tree species for artificial afforestation initiatives in this region since the early 1980s [26]. Geomorphologically, these stands are predominantly distributed across the middle and lower sections of the rocky mountain slopes, occupying an altitudinal range of 149 to 348 m above sea level. The average elevation of the established sample plots is calculated to be 221.5 m. The edaphic conditions across the study sites are relatively uniform, with the soil types consisting mainly of calcareous soils derived from the underlying carbonate parent material [16].

2.2. Sampling Design

To account for the physiological challenges faced by regeneration, particularly the low survival rate of cypress regeneration during the winter season, and to mitigate the confounding effects of climatic interference, the research team conducted extensive field investigations across three distinct periods: July to October 2020, May to June 2021, and a supplementary survey in March 2023. The experimental design employed a stratified

sampling strategy. In the first survey period (July–October 2020), 30 sample plots were established across three representative areas along the Li River with minimal anthropogenic disturbance from tourism: the upper section of Daxu Old Town, the middle section of Yangdi, and the lower section of Xianggong Mountain. In the second survey period (May–June 2021), 6 additional plots were established at two sites in the upper basin near Guilin city: the Forestry Research Institute and Pingfeng.

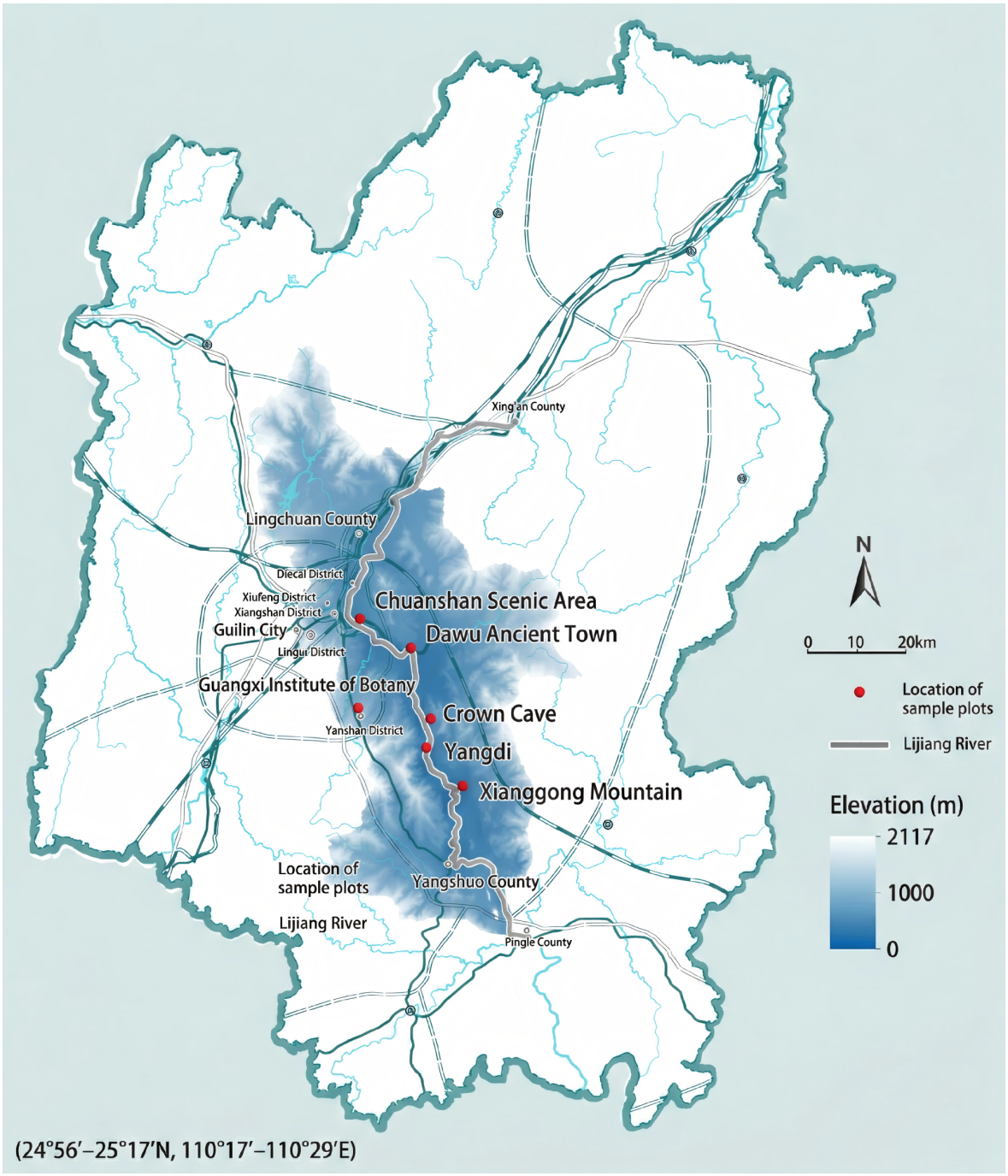


Figure 1. Geographical distribution of the research sample plots within the Lijiang River Basin. Note: The blue color gradient indicates elevation (m a.s.l.). To highlight the spatial distribution of the plots, elevation rendering is restricted to the immediate vicinity of the Lijiang River corridor. White areas denote masked regions outside the study focus and should not be interpreted as zero elevation.

However, during the analysis phase, it was determined that the spatial coverage of the initial 36 plots was insufficient to represent the full range of environmental conditions across

the Li River karst landscape. Consequently, the sampling protocol was adaptively modified. In March 2023, a supplementary survey was conducted, adding 18 plots distributed across six sub-areas: the Yanshan District, including the Guangxi Institute of Botany, Yanshan campus, and Junwu Tomb; the Chuanshan Scenic Area; and additional plots at the existing Daxu and Yangdi sites to increase replication. Through this process, a total of 54 cypress forest research sample plots were established spanning approximately 40 km along the Li River. Each sample plot was standardized as a square quadrat with dimensions of 10 m × 10 m. Each plot was surveyed once; no repeated measurements were conducted. Because the survey period was confounded with geographic location, it could not be meaningfully separated as an independent temporal effect. To assess whether the inclusion of supplementary plots introduced systematic bias, we conducted a sensitivity analysis by comparing the PLS-SEM results obtained from the full dataset ($n = 54$) with those from the initial 36 plots alone. Representative field photographs of the study species and its natural regeneration are shown in Appendix A, Figure A1.

2.3. Data Collection

A systematic and comprehensive investigation was conducted to quantify the natural regeneration status, stand structural attributes (biotic factors), and environmental heterogeneity (abiotic factors) across the sample plots. The data collection followed a rigorous protocol to ensure precision in recording both biological and non-biological variables.

2.3.1. Regeneration Survey

In this study, *Cupressus funebris* individuals with a diameter at breast height (DBH, measured at 1.3 m) of less than 5 cm were defined as regeneration individuals, following the classification criteria of Conner et al. [25] and Xu et al. [29]. For individuals shorter than 1.3 m, ground-line diameter (GLD, measured at the root collar) was recorded as a surrogate metric. These regeneration individuals were stratified into four developmental grades based on height (H): Grade I ($H < 30$ cm), Grade II ($30 \leq H < 60$ cm), Grade III ($60 \leq H < 100$ cm), and Grade IV ($H \geq 100$ cm, GLD or DBH < 5 cm). Following standard terminology in regeneration ecology [30], Grades I–II are hereafter referred to as "seedlings," Grade III as "advanced seedlings," and Grade IV as "saplings." The collective term "regeneration" encompasses all four grades.

2.3.2. Environmental Factors

Four abiotic variables were recorded in each plot. Slope aspect was classified based on azimuth: shaded slopes (0°–45° and 315°–360°), semi-shaded slopes (45°–135°), sunny slopes (135°–225°) and semi-sunny slopes (225°–315°); plots with no discernible inclination were classified as having no aspect [31]. Soil rock fragment content was determined by the excavation method [32]: soil samples of approximately 30–50 cm in thickness were randomly collected, and the volumetric proportion of gravel was measured using the water displacement method. Rock exposure rate was quantified by combining visual estimation with photography [17] and was defined as the ratio of exposed bedrock to the total plot area.

2.3.3. Stand Structure and Understory Characteristics

Nine stand structural and understory variables were measured in each plot. Forest gap area (S) was calculated using the elliptic area formula $S = \pi \times A \times B/4$, where A and B are the long and short axis lengths of the gap, respectively [33]. Canopy closure was assessed using the line-intercept method along the two diagonals of each 10 m × 10 m plot (total transect length: 2×14.14 m ≈ 28.3 m). Along each diagonal, the horizontal projection of all tree crowns intercepting the transect line was recorded, and canopy closure was calculated as the ratio of the cumulative crown intercept length to the total transect

length. Where crown projections overlapped, the overlapping segment was counted only once to avoid overestimation. The same diagonal transect protocol was applied to estimate shrub and herb coverage at the ground level. All visual estimates were conducted by the same two trained observers throughout the study to minimize inter-observer variability; where estimates differed by more than 15%, a consensus value was determined through joint re-examination [34,35].

For understory density, five sub-quadrats were randomly established within each plot, with dimensions of 1 m × 1 m for herbs and 4 m × 4 m for shrubs [36]. Population density (D) was calculated as $D = N/S$, where N is the number of individuals and S is the sampling area. The densities of mature trees and *Cupressus funebris* individuals were determined by a complete census within each plot [37]. Moss coverage was quantified using a combined photographic-visual estimation protocol [38]. In each plot, five randomly positioned 1 m × 1 m quadrats were photographed vertically from a height of 1.5 m using a digital camera (iPhone 13 Pro, Apple Inc., Cupertino, CA, USA) (resolution ≥ 12 MP). Moss-covered area was first estimated visually by two independent observers, and the mean value was adopted. Where discrepancies exceeded 10%, the photograph was analyzed using ImageJ 1.8 (National Institutes of Health, Bethesda, MD, USA) to obtain a reference value. The final moss coverage for each plot was calculated as the arithmetic mean of the five sub-quadrat estimates.

It should be noted that all selected sites were located in areas with minimal recent anthropogenic disturbance, as confirmed by the absence of logging stumps, fire scars, or grazing evidence during field reconnaissance. However, disturbance history was not quantitatively assessed and was therefore not included as a covariate in the analysis.

2.4. Statistical Analysis

All analyses except PLS-SEM were performed in Python 3.11 (Python Software Foundation, Wilmington, DE, USA) using the following libraries: `scikit-bio` and `statsmodels` for RDA, variation partitioning, and permutational ANOVA; `scipy` for Spearman correlations, Kruskal–Wallis tests, and Mann–Whitney U tests; `piecewise-regression` for segmented regression and Davies tests; and `statsmodels` for LOWESS smoothing. PLS-SEM was implemented in SmartPLS 4.1 (SmartPLS GmbH, Oststeinbek, Germany) [39].

2.4.1. Redundancy Analysis and Variation Partitioning

Redundancy analysis (RDA) was performed to quantify the overall explanatory power of environmental and stand structural variables on regeneration composition (Grade I–IV densities as the response matrix). The response matrix was Hellinger-transformed prior to analysis [40]. Model significance was assessed using 999 permutations. Forward selection was applied to rank individual predictors by marginal R^2, and conditional (Type III) effects were tested using permutational ANOVA to evaluate the unique contribution of each variable after controlling for all others. Variation partitioning [41] was subsequently conducted to decompose the explained variance into pure environmental, pure stand structural, and shared fractions.

2.4.2. Partial Least Squares Structural Equation Modeling (PLS-SEM)

Since all variables in this study were directly measured, each was modeled as a single-indicator construct in the PLS-SEM framework, with the indicator loading fixed at 1.0 [42,43]. Variables were selected for the structural equation model based on three criteria: (1) significant correlation with regeneration density (90% BCa confidence interval excluding zero); (2) variance inflation factor (VIF) < 5 to avoid multicollinearity; and (3) theoretical relevance supported by prior literature. A PLS-SEM was constructed to test the hypothesized direct and indirect effects on regeneration density. PLS-SEM was chosen over covariance-based SEM (CB-SEM) for three reasons: (1) the sample size (n = 54) was

relatively small for CB-SEM but adequate for PLS-SEM under the "10-times rule" [44]; (2) ecological data often violate multivariate normality assumptions, which PLS-SEM does not require; and (3) this study was exploratory in nature, aiming to identify key regeneration pathways in a relatively understudied system [45]. Regeneration density was log-transformed [$\ln(x+1)$] prior to analysis, and all variables were standardized to enable comparison of path coefficients.

2.4.3. Threshold Analysis

To identify non-linear breakpoints in the relationships between key predictors and regeneration density, segmented regression was applied to the two dominant predictors (Gap and Ssc) using the method of Muggeo [46]. Breakpoint significance was assessed using the analytical Davies test as implemented in the `piecewise-regression` Python library [47]. For variables where formal breakpoint testing was not feasible due to distributional constraints (moss coverage, herb density, tree density), grouped comparisons (Kruskal–Wallis test with Dunn's post hoc test) and LOWESS smoothing (span = 0.7) were used to characterize response patterns. Slope aspect effects were assessed using Mann–Whitney U tests comparing shady versus sunny slopes.

2.5. Ethical Considerations

This study scrupulously complies with all pertinent ethical guidelines and regulations governing academic research. It is hereby confirmed that prior to the commencement of this research, the protocol received internal review and approval from the relevant institutional bodies, with the corresponding ethics review forms attached. The ethical compliance is articulated through the following dimensions:

Fundamentally, this research is designated as a foundational ecological field survey, with the primary objective of systematically observing, measuring, and collecting empirical data from the natural environment. Regarding biological subjects, it is explicitly declared that the experimental design involved neither human participants nor animal experimentation, thereby exempting it from clinical ethical review. Crucially, the methodological framework of this research relied strictly on non-invasive observation to assess the regeneration processes of cypress communities. All fieldwork was conducted using non-destructive sampling protocols, involving only the visual assessment of non-protected species and the collection of minimal substrate samples (e.g., soil, litter) for laboratory analysis, ensuring that no ecological damage was inflicted upon the existing vegetation or the local habitat.

3. Results

3.1. Structural Composition of Regeneration Individuals

3.1.1. Density Structure of Regeneration

The investigation revealed a highly heterogeneous pattern of natural regeneration within the *Cupressus funebris* stands, which are predominantly distributed across the middle and lower elevational zones (149–348 m) of the rocky mountains. The studied stands, comprising both pure and mixed cypress forests with a diameter at breast height (DBH) ranging from 10 to 25 cm, exhibited significant variability in regeneration density. As illustrated in Figure 2, a substantial proportion of the surveyed plots (23 out of 54, representing 42.6%) exhibited a complete failure of recruitment, with a recorded regeneration density of 0 plants ha^{-1}. Among the 31 plots with regeneration, one exceptional plot (Plot 8) demonstrated a prolific regeneration event, achieving a density as high as 48,600 plants ha^{-1}. The remaining 30 plots displayed a broad density spectrum ranging from 1 to 8000 plants ha^{-1}.

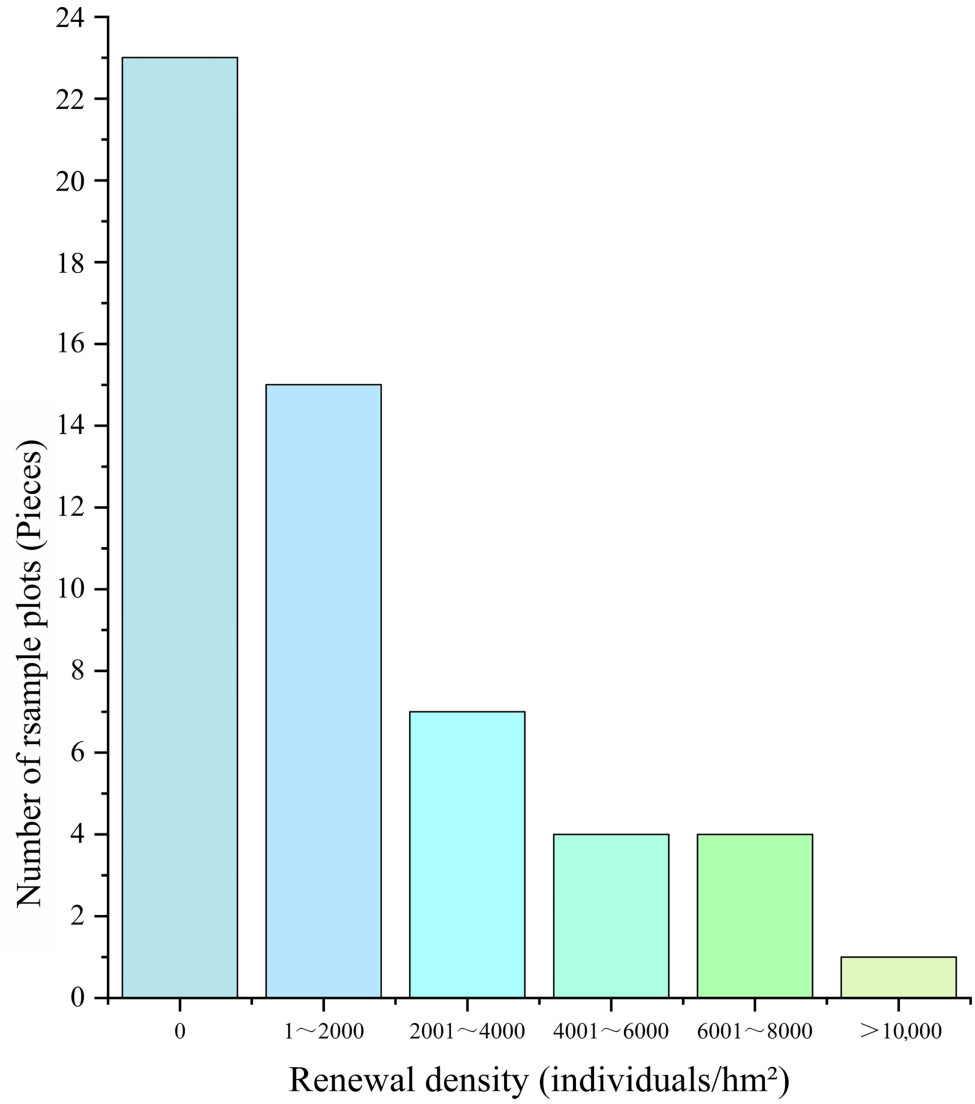


Figure 2. Distribution of cypress seedling density across the 54 surveyed sample plots.

3.1.2. Height Class Structure and Demographic Dynamics

Height class distribution serves as a reliable proxy for demographic structure when precise age data are unavailable [29]. Natural regeneration of *Cupressus funebris* was recorded in 31 of the 54 plots (57.4%), while the remaining 23 plots exhibited no regeneration. All 54 plots, including those with zero regeneration, were retained for the subsequent PLS-SEM analysis to avoid selection bias and to capture the full range of environmental variation. For the height class characterization, Plot 8 was excluded only for the height-class characterization; it was retained in all subsequent analyses.

As depicted in Figure 3, the height class distribution of the regenerated population displayed a distinct inverted J shape, characterized by a progressive decline in abundance with increasing height class. Seedling abundance differed significantly between Grade I and Grade III, and between Grade I and Grade IV (Kruskal–Wallis test followed by Dunn's post hoc test, $p < 0.05$), whereas no significant differences were detected among the remaining pairwise comparisons. Grade I seedlings (establishment phase) were the most abundant, suggesting that seed availability and initial germination conditions are not the primary limiting factors. However, the sharp attrition observed in subsequent height classes indicates that seedlings encounter intensifying environmental filters and

competitive pressures during ontogenetic development, which severely constrain their recruitment into the sapling layer.

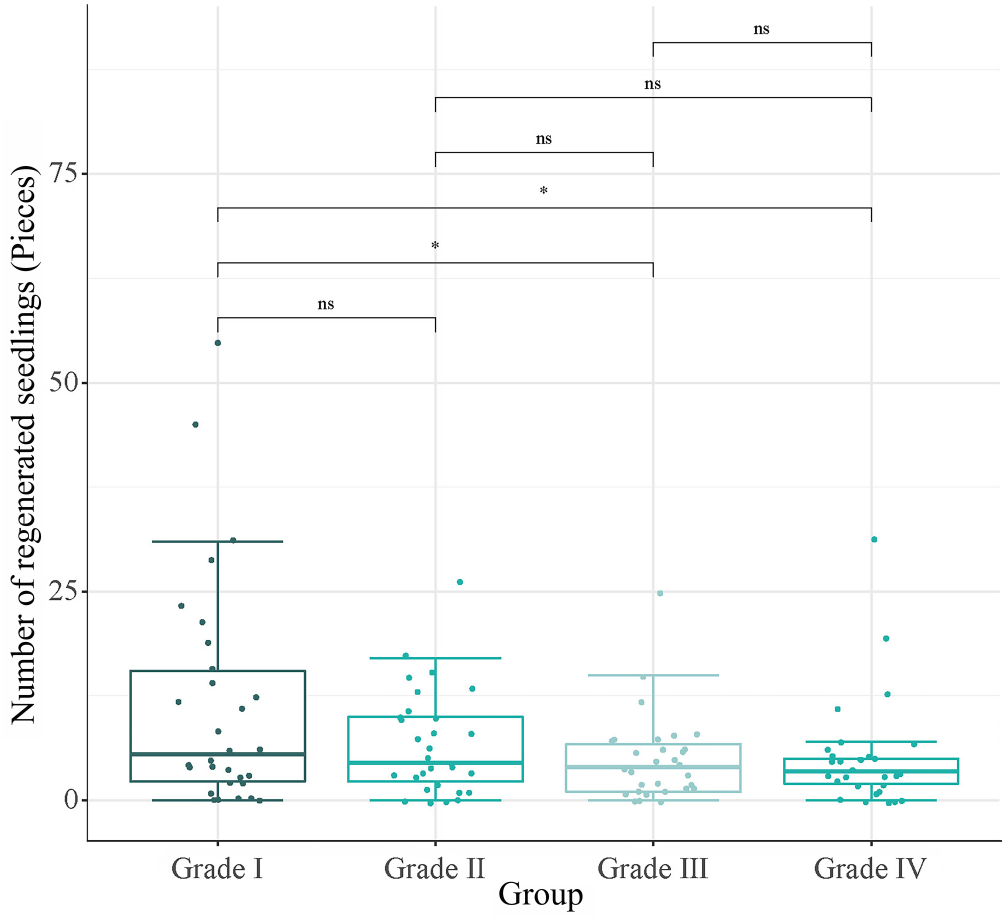


Figure 3. Height class structure of regenerated cypress seedlings, illustrating a progressive demographic bottleneck. Note: Horizontal brackets indicate pairwise comparisons among grades based on Dunn's post hoc test following the Kruskal–Wallis test. * indicate statistically significant differences at $p < 0.05$; "ns" indicates non-significant differences.

3.2. Descriptive Statistics of Environmental and Stand Variables

The descriptive statistics of all predictor variables are summarized in Table 1. The sampled plots spanned an elevational range of 149–348 m (CV = 15.387%), while edaphic variables exhibited considerably greater heterogeneity: rock exposure rate ranged from 0 to 70% (CV = 108.378%) and soil rock fragment content from 0 to 51% (CV = 216.826%), reflecting the pronounced substrate variability inherent to karst terrain. *Cupressus funebris* constituted 80.6% of total tree density (1027.780 of 1275.930 stems ha^{-1}), confirming its numerical dominance across the study stands. Canopy closure varied from 5.000% to 98.000% (CV = 52.051%), and forest gap area from 0 to 86.250 m^2 (CV = 118.057%), indicating a structural continuum from closed-canopy to gap-dominated conditions. The understory was co-dominated by herbs (53.815 ± 23.984%) and shrubs (40.133 ± 27.133%), while moss coverage was low but highly variable (CV = 110.648%). Combined with the extreme spatial heterogeneity in seedling density documented previously, these gradients provide a sufficient basis for identifying the key drivers of cypress regeneration in the subsequent multivariate analyses.

Table 1. Descriptive statistics of environmental factors, stand structure, and regeneration variables.

Category	Variable	Abbreviation	Unit	Mean ± SD	Min–Max	CV (%)
Environmental factors	Elevation	Al	m	215.944 ± 33.228	149–348	15.387
	Slope	S	°	16.093 ± 12.641	0–48	78.549
	Rock exposure rate	R	%	17.769 ± 19.257	0–70	108.378
	Soil rock fragment content	Ssc	%	4.296 ± 9.315	0–51	216.826
Stand structure & understory	Tree density	TreeDen	stems ha^{-1}	1275.930 ± 1198.730	200–6200	93.950
	Cupressus funebris density	CypDen	stems ha^{-1}	1027.780 ± 1085.130	100–6200	105.580
	Canopy closure	CC	%	55.463 ± 28.869	5–98	52.051
	Forest gap area	Gap	m^2	13.648 ± 16.112	0–86.25	118.057
	Shrub coverage	ShrubCov	%	40.133 ± 27.133	0–99	67.606
	Shrub density	ShrubDen	stems ha^{-1}	7112.960 ± 4717.760	0–25,300	66.326
	Herb coverage	HerbCov	%	53.815 ± 23.984	8–99	44.567
	Herb density	HerbDen	stems ha^{-1}	10,497.220 ± 5267.980	2700–26,500	50.185
	Moss coverage	MossCov	%	22.870 ± 25.306	0–80	110.648
Regeneration	Grade I ($H < 30$ cm)	GradeI	stems ha^{-1}	942.593 ± 2217.480	0–14,600	235.253
	Grade II ($30 \leq H < 60$ cm)	GradeII	stems ha^{-1}	600.000 ± 1783.150	0–12,800	297.192
	Grade III ($60 \leq H < 100$ cm)	GradeIII	stems ha^{-1}	477.778 ± 1515.910	0–10,900	317.284
	Grade IV ($H \geq 100$ cm, DBH < 5 cm)	GradeIV	stems ha^{-1}	464.815 ± 1466.890	0–10,300	315.585

Note: Slope aspect was recorded as a categorical variable and is summarized separately: shaded slopes ($n = 11$), semi-shaded slopes ($n = 12$), sunny slopes ($n = 9$), semi-sunny slopes ($n = 10$), and flat terrain ($n = 12$).

3.3. Correlation Analysis

3.3.1. Correlation Analysis: Environmental Drivers

Spearman rank correlation analysis was performed in order to disentangle the relationships between abiotic environmental factors and seedling demographics (Figure 4). As slope aspect is a circular variable that cannot be meaningfully analyzed using linear correlation methods [48], it was treated as a categorical factor in all analyses. Differences in regeneration related to aspect were assessed using the Kruskal–Wallis test. The analysis revealed a significant positive correlation between altitude (Al) and slope (S) on the one hand, and Grade II–IV regeneration individuals on the other ($p \leq 0.05$). Furthermore, the correlation strength increased progressively from smaller to larger size classes (Al: $\rho = 0.344$–0.363; S: $\rho = 0.254$–0.361). This suggests that topographic positioning becomes increasingly critical for the survival of larger saplings. It is noteworthy that neither variable demonstrated a significant correlation with Grade I seedlings, suggesting that the filtering effect of topography intensifies during later ontogenetic stages.

The analysis also revealed a robust positive correlation between soil rock fragment content (Ssc) and ontogenetic stage (Grades I–IV, $p \leq 0.01$), with the strongest association observed for Grade I seedlings ($\rho = 0.554$). This finding underscores the unique adaptation of *Cupressus* to rocky microsites and highlights the particular importance of well-drained substrates during the initial establishment phase. Conversely, rock exposure rate (R) exhibited no substantial correlation with any regeneration grade ($\rho = -0.001$–0.068, $p > 0.1$), indicating that surface rock exposure per se may not exert a significant influence on *Cupressus* regeneration. Collectively, these results suggest that soil rock fragment content, altitude, and slope gradient are positively associated with *Cupressus* regeneration, and may serve as important abiotic filters shaping regeneration patterns in karst landscapes.

3.3.2. Correlation Analysis: Biotic Drivers

The Spearman correlation matrix for stand structural factors (Figure 5) revealed a complex network of biotic associations with regeneration density. Among all biotic variables, gap area (Gap) exhibited the strongest positive correlations with regeneration density across all size classes ($\rho = 0.711$–0.791, $p \leq 0.01$), with the highest coefficient observed

for Grade I seedlings ($\rho = 0.791$). This suggests that canopy openings may serve as critical recruitment windows, particularly during the initial establishment phase when light demand is presumably highest. Moss coverage (MossCov) displayed consistently strong positive correlations with all seedling grades ($\rho = 0.676$–0.764, $p \leq 0.01$), with the association strengthening towards larger size classes (Grade IV: $\rho = 0.764$). This pattern may reflect shared microhabitat preferences characterized by moderate moisture retention and reduced competition. *Cupressus* density (CypDen) demonstrated a positive correlation with both Grade II ($\rho = 0.309$, $p \leq 0.05$) and Grade III advanced seedlings ($\rho = 0.320$, $p \leq 0.05$), suggesting a potential association with proximity to seed sources. However, this correlation became non-significant for Grade IV saplings ($\rho = 0.176$, $p > 0.1$), which could be indicative of density-dependent thinning at subsequent ontogenetic stages.

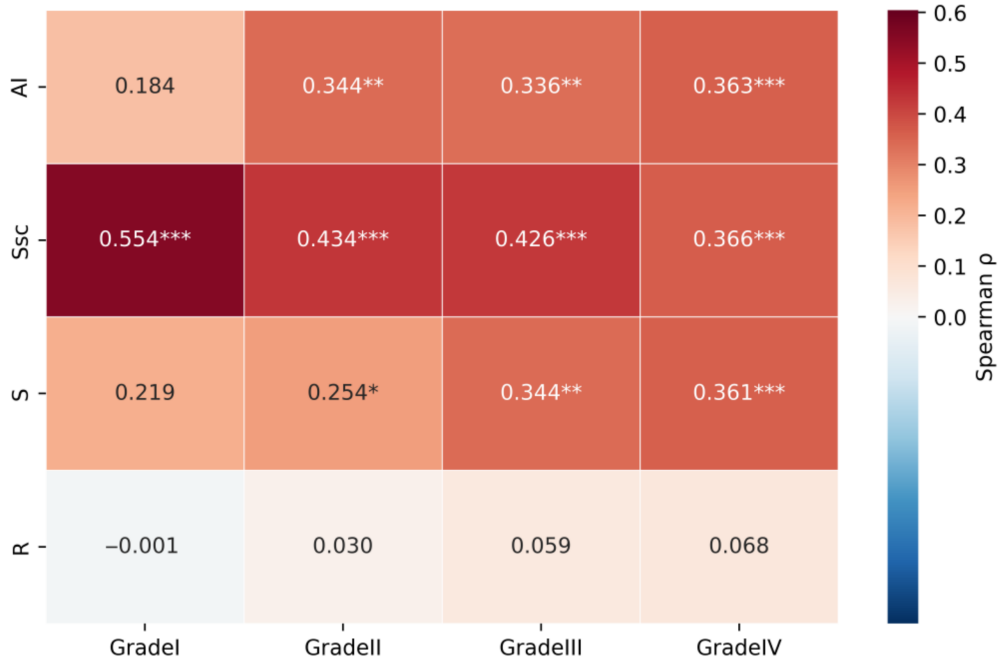


Figure 4. Heatmap of Spearman correlation coefficients between environmental factors and cypress seedling grades. Note: Al: Altitude; Ssc: Soil stone content; S: Slope; R: Rock exposure rate; Grade I–IV: Seedling height classes. *, **, and *** denote significance at $p \leq 0.1$, $p \leq 0.05$, and $p \leq 0.01$, respectively.

Conversely, several variables exhibited negative correlations, suggesting competitive interactions. The study revealed a negative correlation between herbal density (HerbDen) and all four regeneration grades ($\rho = -0.315$ to -0.363, $p \leq 0.05$). A similar pattern was observed in the relationship between herb coverage (HerbCov) and regeneration grades ($\rho = -0.227$ to -0.291, $p \leq 0.1$ for most grades). These findings provide evidence that the herbaceous layer may exert consistent competitive pressure during the regeneration process. Canopy closure (CC) exhibited a significant negative correlation exclusively with Grade IV saplings ($\rho = -0.304$, $p \leq 0.05$), implying that light limitation may become increasingly critical as individuals transition from seedling to sapling stages and their resource demands escalate. Tree density (TreeDen) of non-*Cupressus* species exhibited marginally negative associations with Grade I ($\rho = -0.259$, $p \leq 0.1$) and Grade IV saplings ($\rho = -0.256$, $p \leq 0.1$), suggesting the possibility of interspecific competition. However, the relatively weak correlations necessitate cautious interpretation. The findings indicated that neither shrub coverage (ShrubCov) nor shrub density (ShrubDen) exhibited a significant correlation with any regeneration grade ($p > 0.1$ for all), suggesting that the shrub layer does not play a detectable role in *Cupressus* regeneration within the study area. Collectively,

these correlation patterns delineate a biotic environment in which light availability and microhabitat conditions appear to be positively linked to regeneration success, while herbaceous competition emerges as a consistent negative correlate. These correlative findings provide a foundation for subsequent modeling efforts aimed at disentangling the relative contributions of individual factors.

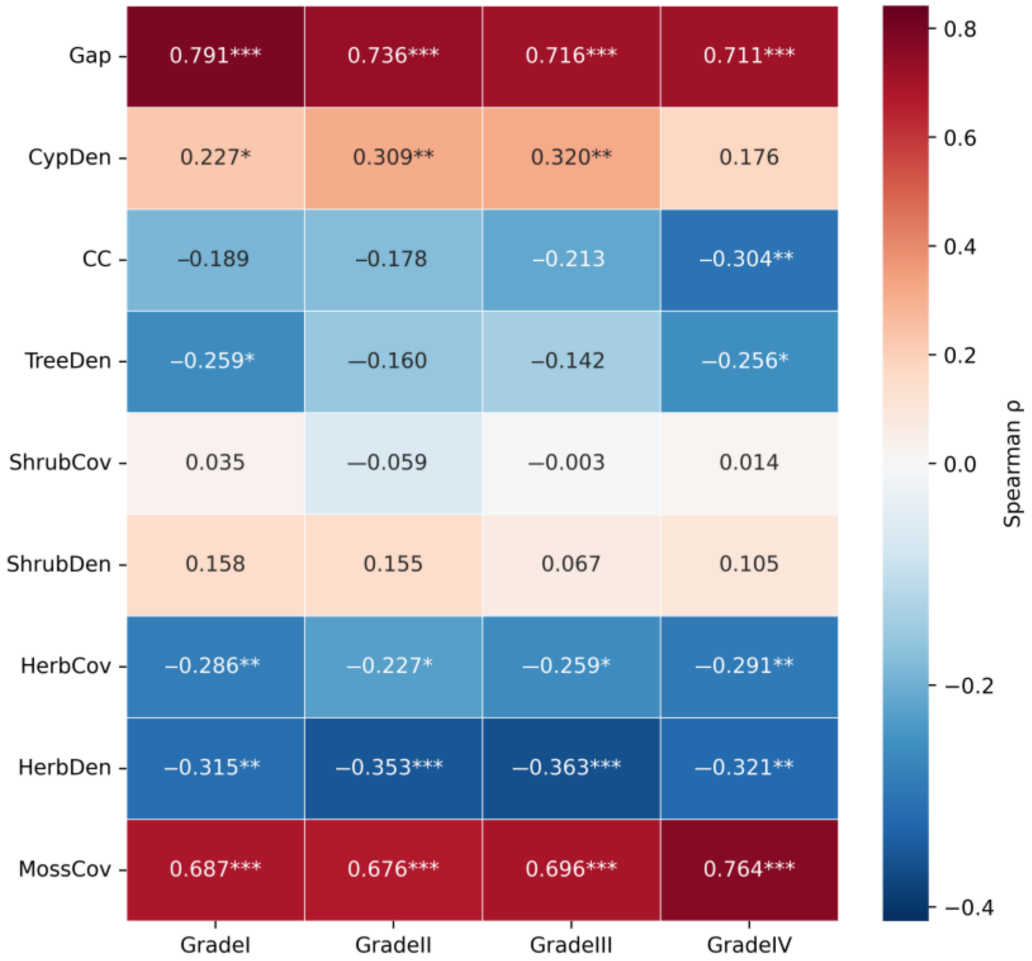


Figure 5. Heatmap of Spearman correlation coefficients between stand structural factors and cypress seedling grades. Note: Gap: Gap area; CypDen: Cypress density; CC: Canopy closure; TreeDen: Tree density; ShrubCov: Shrub coverage; ShrubDen: Shrub density; HerbCov: Herbal coverage; HerbDen: Herbal density; MossCov: Moss coverage. *, **, and *** denote significance at $p \leq 0.1$, $p \leq 0.05$, and $p \leq 0.01$, respectively.

3.4. Drivers of Cupressus Regeneration

To identify the key factors influencing *Cupressus* regeneration patterns, redundancy analysis (RDA) was performed using all environmental and stand structure variables as explanatory factors. The full RDA model significantly explained 74.3% of the total variation in regeneration composition (adjusted $R^2 = 0.659$, $p = 0.002$; Table 2). The first canonical axis (RDA1) accounted for 97.7% of the constrained variance and was highly significant ($p = 0.001$), while the remaining axes contributed minimally (RDA2–4: 2.3% combined, all $p > 0.05$), indicating that a single dominant gradient structured the regeneration–environment relationship.

Table 2. Summary of RDA on *Cupressus* regeneration constrained by environmental and stand structure variables.

Axis	Eigenvalue	Variance Explained (%)	Cumulative Variance (%)	*p*-Value
RDA1	2.959	97.7	97.7	0.001 ***
RDA2	0.053	1.7	99.4	0.886
RDA3	0.016	0.5	99.9	0.792
RDA4	0.001	0	100	0.314
Total Constrained		74.29		
Unconstrained		25.71		
Model fit R^2		0.743		
Adjusted R^2		0.659		0.002 ***

Note: Significance was tested using 999 permutations. *** $p < 0.01$.

Forward selection was then applied to identify the most influential predictors (Table 3), and this method inherently addresses multicollinearity by sequentially adding variables based on their marginal contribution after accounting for previously selected predictors [49]. Among all variables examined, Soil stone content (Ssc) emerged as the strongest driver, independently explaining 52.9% of regeneration variation ($p = 0.001$). Canopy gap ratio (Gap) ranked second, contributing an additional 11.9% to the explained variance ($p = 0.001$). Other significant variables included shrub density (4.1%), shrub coverage (2.4%), and moss coverage (0.4%), though their individual contributions were considerably smaller. Notably, all 13 variables retained in the final model showed significant marginal effects ($p = 0.001$ for all). However, when the conditional effects of individual variables were tested using permutational ANOVA, a contrasting pattern emerged. After controlling for all other predictors, only Rock exposure rate (R, conditional $R^2 = 0.040$, $p = 0.038$) and moss coverage (MossCov, conditional $R^2 = 0.039$, $p = 0.038$) retained significant unique contributions (see in Appendix A, Table A1).

Table 3. Forward selection of environmental and stand structure variables in RDA.

Variable	Category	Marginal R^2	Cumulative R^2	*p*-Value
Ssc	Environmental	0.529	0.529	0.001 ***
Gap	Stand structure	0.119	0.648	0.001 ***
ShrubDen	Stand structure	0.041	0.689	0.001 ***
ShrubCov	Stand structure	0.024	0.713	0.001 ***
HerbCov	Stand structure	0.006	0.719	0.001 ***
TreeDen	Stand structure	0.005	0.724	0.001 ***
HerbDen	Stand structure	0.005	0.729	0.001 ***
MossCov	Stand structure	0.004	0.733	0.001 ***
Al	Environmental	0.004	0.737	0.001 ***
CypDen	Stand structure	0.003	0.740	0.001 ***
S	Environmental	0.002	0.742	0.001 ***
CC	Stand structure	0.002	0.744	0.001 ***
R	Environmental	0.001	0.745	0.001 ***

Note: Al: Altitude; Ssc: Soil stone content; S: Slope; R: Rock exposure rate; Gap: Gap area; CypDen: Cypress density; CC: Canopy closure; TreeDen: Tree density; ShrubCov: Shrub coverage; ShrubDen: Shrub density; HerbCov: Herbal coverage; HerbDen: Herbal density; MossCov: Moss coverage. *** $p < 0.01$.

To further disentangle the relative importance of environmental versus stand structure factors, variation partitioning analysis was conducted (Table 4; Figure 6). The results revealed that the shared fraction explained by both factor groups (41.2%) substantially exceeded their unique contributions (environmental factors alone: 8.6%; stand structure alone: 16.2%). Both the environmental model and stand structure model were individually significant. The residual unexplained variation accounted for 34.1% of total variance,

likely reflecting stochastic processes and unmeasured factors such as seed availability and herbivory pressure.

Table 4. Variation partitioning of *Cupressus* regeneration explained by environmental factors and stand structure variables.

Component	Notation	Adjusted R^2
Environmental	[a]	0.086 ***
Stand structure	[b]	0.162 ***
Shared	[ab]	0.412
Environmental (total)	[a] + [ab]	0.498 ***
Stand structure (total)	[b] + [ab]	0.574 ***
Full model	[a] + [b] + [ab]	0.659 ***
Residual		0.341

Note: Variation partitioning was performed following Borcard et al. [41]. Values represent the proportion of adjusted explained variation. [a]: pure environmental effect; [b]: pure stand structure effect; [ab]: shared effect; Residual: unexplained variation. Significance of the pure fractions [a] and [b], total fractions, and the full model was assessed using 999 permutations. The shared fraction [ab] was calculated by subtraction and cannot be tested directly. *** $p < 0.01$.

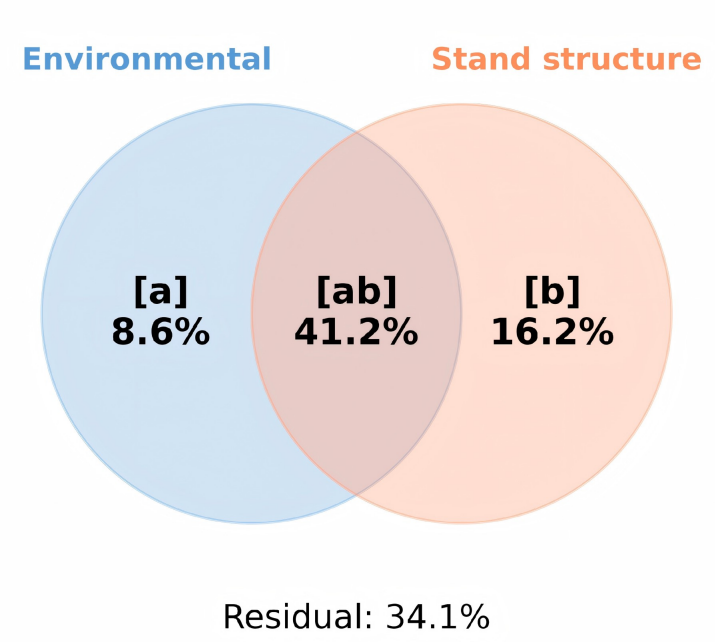


Figure 6. Variation Partitioning. Note: Values represent the percentage of adjusted explained variation. [a]: pure environmental effect; [b]: pure stand structure effect; [ab]: shared effect; Residual: unexplained variation. All fractions were significant at $p < 0.01$ based on 999 permutations.

The RDA triplot provided insights into the ecological associations between regeneration grades and environmental gradients (Figure 7). Along the primary axis (RDA1), Grade I seedlings (height < 30 cm) were positively associated with canopy gaps and positioned toward the right side of the ordination space, suggesting that light availability is a critical factor for initial seedling establishment. In contrast, larger regeneration classes (Grade II–IV) showed stronger positive correlations with Soil stone content (Ssc) and moss coverage (MossCov), indicating shifting microhabitat requirements across ontogenetic stages. Conversely, tree density (TreeDen), herb layer density (HerbDen), and canopy coverage (CC) were negatively associated with all regeneration grades along RDA1, implying competitive suppression effects from dense overstory and understory vegetation on *Cupressus* regeneration success.

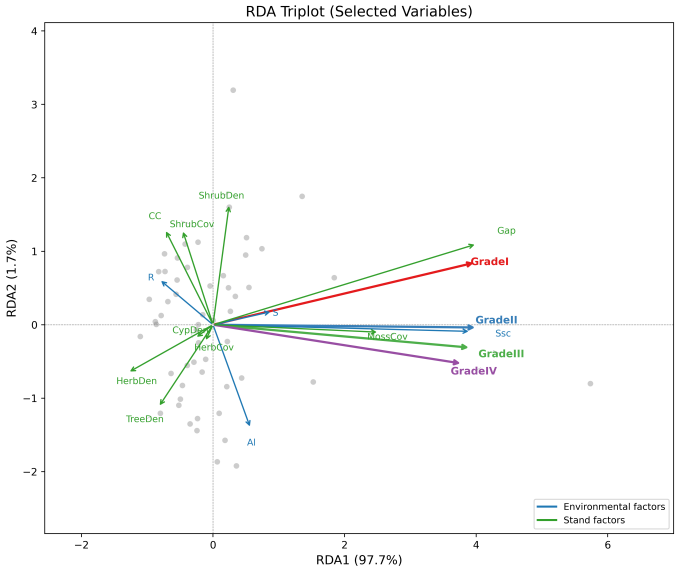


Figure 7. RDA Triplot. Note: The first two RDA axes explained 99.4% of the total constrained variance. Regeneration grades are color-coded: red (Grade I) represents the youngest seedlings ($H < 30$ cm); purple (Grade IV) represents advanced saplings ($H \geq 100$ cm, DBH < 5 cm); blue (Grade II) and green (Grade III) represent intermediate stages. Environmental factors (blue arrows) and stand structural factors (green arrows) are displayed with their abbreviated variable names. Gray points represent sampling plots.

3.5. Structural Equation Modeling

Partial least squares structural equation modeling (PLS-SEM) was employed to disentangle the direct and indirect effects of environmental and stand structural factors on *Cupressus funebris* regeneration (Figure 8). The model comprised three latent variables: environmental factors (ENV), stand structure (STAND), and regeneration (REGEN). ENV and STAND were specified as formative constructs, while REGEN was modeled as a reflective construct. The hypothesized causal pathway assumed that ENV influences REGEN both directly and indirectly through STAND.

3.5.1. Measurement Model Assessment

For the reflective construct REGEN, all four indicator loadings exceeded 0.93 (Grade I: 0.932, Grade II: 0.988, Grade III: 0.985, Grade IV: 0.967; all $p < 0.001$; Table 5), indicating excellent internal consistency and convergent validity. All VIF values were below 5.0 (see in Appendix A, Table A2), confirming the absence of critical multicollinearity among formative indicators [42].

For the formative constructs, outer weights and loadings were examined to evaluate indicator contributions (Table 5, Appendix A, Table A3). In the ENV construct, soil rock fragment content (Ssc) was the dominant contributor with a significant weight (0.963, $p < 0.01$) and loading (0.984, $p < 0.001$), while slope (S) showed a marginally significant loading (0.328, $p = 0.051$). Altitude (Al) and rock exposure rate (R) showed non-significant outer loadings. However, these indicators were retained based on their theoretical relevance as key environmental gradients identified in the RDA and variation partitioning analyses (see Sections 3.3 and 3.4). In the STAND construct, canopy gap fraction (Gap) was the primary contributor with a significant loading (weight = 1.091, $p < 0.001$; loading = 0.989, $p < 0.001$). Moss coverage (loading = 0.676, $p < 0.001$) and herb density (loading = -0.282, $p = 0.001$) also showed significant loadings, supporting their retention in the model [42].

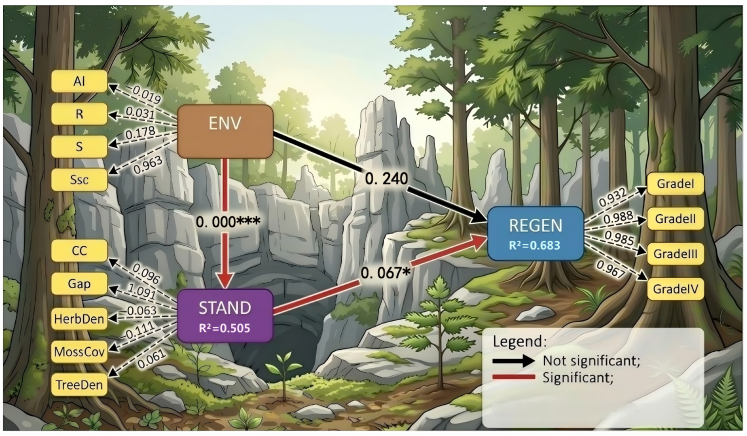


Figure 8. PLS-SEM: Effects of environmental factors and stand structure on the regeneration of *Cupressus funebris* in karst landscapes of the Li River basin. Note: The visual karst background for this figure was generated with an AI-assisted image tool. All path coefficients and R^2 values are derived from empirical data analyzed with SmartPLS 4.1 (SmartPLS GmbH, Oststeinbek, Germany) and are separate from the conceptual backdrop. This generated element is for illustrative purposes only and does not represent original data. ENV and STAND are specified as formative constructs; REGEN is specified as a reflective construct. Values adjacent to indicator arrows represent outer weights. Values on structural paths denote p-values. Red arrows indicate statistically significant paths; black arrows indicate non-significant paths. R^2 values within STAND and REGEN represent the variance explained by the model. * $p < 0.1$, *** $p < 0.01$.

Table 5. Measurement model results of PLS-SEM.

Construct	Indicator	Outer Loading	*t*-Value	*p*-Value
ENV	Al	0.126	0.660	0.509
	R	−0.111	0.701	0.484
	S	0.328	1.949	0.051 *
	Ssc	0.984	4.959	<0.001 ***
STAND	CC	−0.115	0.713	0.476
	Gap	0.989	14.184	<0.001 ***
	HerbDen	−0.282	3.202	0.001 ***
	MossCov	0.676	5.875	<0.001 ***
	TreeDen	−0.167	1.808	0.071 *
REGEN	Grade I	0.932	6.943	<0.001 ***
	Grade II	0.988	18.715	<0.001 ***
	Grade III	0.985	18.758	<0.001 ***
	Grade IV	0.967	8.659	<0.001 ***

Note: ENV: Environmental factors; STAND: Stand Structure factors; REGEN: Regeneration factors; Al: Altitude; Ssc: Soil stone content; S: Slope; R: Rock exposure rate; Gap: Gap area; CC: Canopy closure; TreeDen: Tree density; HerbDen: Herbal density; MossCov: Moss coverage; Grade I–IV: Regeneration individuals height classes. * $p < 0.1$, *** $p < 0.01$.

3.5.2. Structural Model Assessment

The model exhibited a satisfactory fit, as evidenced by a standardized root mean square residual (SRMR) of 0.056, which was significantly below the recommended threshold of 0.08 [50]; Table 6. The model accounted for 50.5% of the variance in STAND ($R^2 = 0.505$, $p = 0.002$) and 68.3% of the variance in REGEN ($R^2 = 0.683$, $p < 0.001$), suggesting considerable explanatory capacity (Table 6).

Path analysis revealed that ENV exerted a strong and significant positive effect on STAND ($\beta = 0.711$, $t = 4.158$, $p < 0.001$), while STAND showed a marginally significant positive effect on REGEN ($\beta = 0.499$, $t = 1.830$, $p = 0.067$). Notably, the direct effect of ENV on REGEN was not significant ($\beta = 0.394$, $t = 1.174$, $p = 0.240$; Figure 8, Table 6).

Table 6. Structural model results: path coefficients, indirect and total effects.

Path	Effect Type	β	SE	t-Value	p-Value
ENV → STAND	Direct	0.711	0.171	4.158	<0.001 ***
ENV → REGEN	Direct	0.394	0.335	1.174	0.240
STAND → REGEN	Direct	0.499	0.273	1.830	0.067 *
ENV → STAND → REGEN	Indirect	0.355	0.198	1.790	0.073 *
ENV → REGEN	Total	0.748	0.219	3.420	0.001 ***
Endogenous variable	R^2	SE	t-value	p-value	
STAND	0.505	0.163	3.099	0.002 ***	
REGEN	0.683	0.117	5.847	<0.001 ***	
Model fit	Value				
SRMR	0.056				

Note: ENV: Environmental factors; STAND: Stand Structure factors; REGEN: Regeneration factors; * $p < 0.1$, *** $p < 0.01$.

3.5.3. Mediation Analysis

The indirect effect of ENV on REGEN through STAND was 0.355 ($t = 1.790$, $p = 0.073$), accounting for 47.5% of the total effect. The total effect of ENV on REGEN was 0.748 ($t = 3.420$, $p = 0.001$), which was highly significant despite the non-significant direct path. This pattern, with a significant total effect, a significant a-path (ENV → STAND), a marginally significant b-path (STAND → REGEN), and a non-significant direct effect (c'-path), is consistent with full mediation [42,51]. These results indicate that environmental factors primarily influence *Cupressus funebris* regeneration indirectly by shaping stand structural attributes, rather than through direct effects on seedling establishment (Figure 8, Table 6). To assess the robustness of the PLS-SEM results, a sensitivity analysis was performed utilizing a subset of 36 plots from the preliminary survey; the results, which were consistent with those obtained from the full dataset ($n = 54$), are presented in Appendix A, Figure A2 and Table A4.

3.6. Threshold Identification for Key Regeneration Drivers

In order to complement the continuous relationships identified by RDA and PLS-SEM, threshold effects of key predictors on regeneration density were examined using segmented regression, non-parametric group comparisons, and LOWESS smoothing.

For the canopy gap area, segmented regression identified a significant breakpoint at 10.49 m^2 (95% CI: 6.42–14.57 m^2; Davies test, $p = 0.028$). Below this threshold, regeneration density exhibited a steep increase in proportion to gap area (slope $\alpha_1 = 0.579$, $p < 0.001$), while above the threshold, the relationship reached a state of plateau (slope $\alpha_2 = 0.052$, $p = 0.079$). The segmented model ($R^2 = 0.654$) substantially outperformed the linear model ($R^2 = 0.440$), confirming the non-linear nature of the gap–regeneration relationship. The results of the grouped comparison confirmed this pattern: the mean total seedling density rose sharply from 327 stems per hectare in the 0–5 m^2 ($n = 21$) to 7133 stems per hectare in the >20 m^2 class ($n = 14$; Kruskal–Wallis test for Grade I, $p < 0.001$; Figure 9a), with the transition being most pronounced between the 5–10 m^2 and 10–20 m^2 classes, consistent with the estimated breakpoint.

The Davies test detected a significant breakpoint for soil rock fragment content ($p < 0.001$), with an estimated breakpoint of Ssc ≈ 3.96% (95% CI: −0.96% to 8.88%). However, the wide confidence interval spanning zero, coupled with the non-significant pre-breakpoint slope ($\alpha_1 = 0.887$, $p = 0.100$), suggests that this signal was primarily driven by the contrast between plots with and without rock fragments, rather than indicating a precise dose–response threshold. Applying segmented regression to the non-zero subset (Ssc > 0, $n = 33$; Table 7) yielded a non-significant Davies test ($p = 0.052$), which confirmed the absence of a breakpoint within the Ssc > 0 range. However, a simple linear model for this subset was significant ($R^2 = 0.147$,

$p = 0.027$, slope = 0.115), which indicates a weak but positive continuous effect beyond the dominant presence–absence effect. Therefore, the effect of rock fragments operated as a binary presence–absence mechanism: plots with Ssc > 0 supported significantly higher regeneration density than plots with Ssc $= 0$ across all seedling grades (Mann–Whitney U tests: Grade I: $p < 0.001$; Grade II: $p < 0.01$; Grade III: $p < 0.01$; Grade IV: $p < 0.05$; Figure 9b).

Table 7. Segmented regression of ln-transformed regeneration density on canopy gap area and soil rock fragment content.

Variable	Dataset	Analysis	Estimate	SE	95% CI	*p*-Value
Gap	Full ($n = 54$)	Davies test	—	—	—	0.028
		Breakpoint	10.49 m^2	2.04	[6.42, 14.57]	—
		Slope before BP (α_1)	0.579	—	—	< 0.001
		Slope after BP (α_2)	0.052	—	—	0.079
		Segmented model R^2	0.654	—	—	—
		Linear model R^2	0.440	—	—	—
Ssc	Full ($n = 54$)	Davies test	—	—	—	< 0.001
		Breakpoint	3.96%	2.45	[−0.96, 8.88]	—
		Slope before BP (α_1)	0.887	0.529	[−0.18, 1.94]	0.100
		Slope after BP (α_2)	0.073	0.058	[−0.04, 0.19]	0.218
		Segmented model R^2	0.259	—	—	—
		Linear model R^2	0.159	—	—	—
	Non-zero subset ($n = 33$)	Davies test	—	—	—	0.052
		Breakpoint	3.90%	3.29	[−2.82, 10.62]	—
		Slope before BP (α_1)	0.912	1.170	[−1.47, 3.29]	0.440
		Slope after BP (α_2)	0.073	0.057	[−0.04, 0.19]	0.209
		Segmented model R^2	0.216	—	—	—
		Linear model R^2	0.147	—	—	0.027

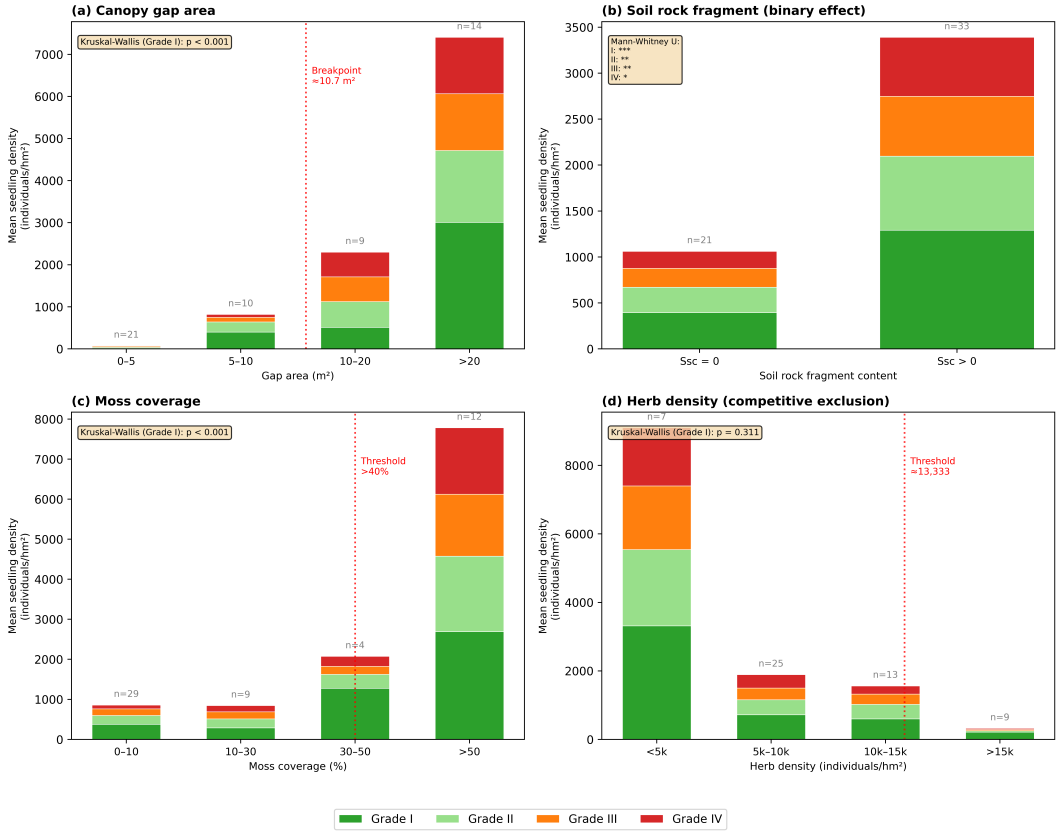


Figure 9. Threshold identification. (**a**) Canopy gap area; (**b**) Soil rock fragment content; (**c**) Moss coverage; (**d**) Herb layer density. Note: *, **, and *** denote significance at $p \leq 0.1$, $p \leq 0.05$, and $p \leq 0.01$, respectively.

Among the remaining stand structural variables, regeneration density increased monotonically with moss coverage, accelerating markedly above approximately 40% (Figure 9c). Plots with moss coverage of over 50% ($n = 12$) had mean seedling densities around eight times higher than those with coverage of under 10% ($n = 29$; Kruskal–Wallis test for Grade I, $p < 0.001$). This suggests that extensive moss mats create favorable microsites for seed retention and germination. Regeneration density peaked at intermediate herb densities (<5000 stems ha^{-1}) and declined progressively at higher densities, with near-complete suppression at herb densities exceeding approximately 13,000 stems ha^{-1} (Figure 9d); although the Kruskal–Wallis test for Grade I seedlings was not significant ($p = 0.311$), likely due to the small sample size in the highest density class ($n = 9$), the consistent decline across all grades suggests a competitive exclusion effect. LOWESS smoothing of Grade I seedling density against tree density revealed a hump-shaped response (Figure 10), with regeneration highest at tree densities of 500–1500 stems ha^{-1} and consistently suppressed below 300 stems ha^{-1} beyond a competitive exclusion threshold of approximately 2200 stems ha^{-1}, reflecting intensified competition for light, water, and nutrients under dense canopy closure.

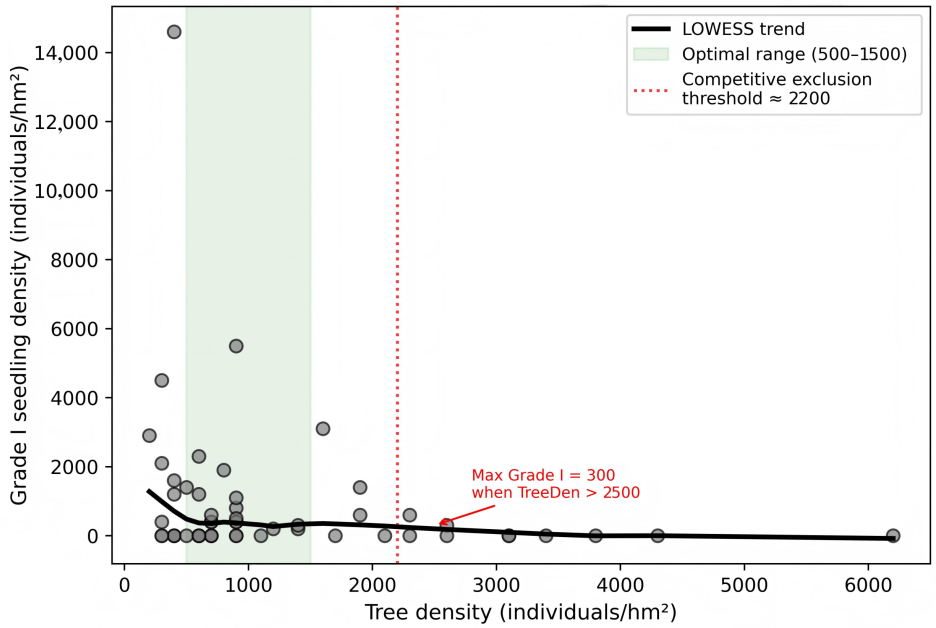


Figure 10. Tree density regulation (Grade I scatter + LOWESS).

Regarding slope orientation, shady (north-facing) slopes supported significantly higher seedling densities than sunny (south-facing) slopes across all developmental grades (Mann–Whitney U tests: Grade I, $p = 0.007$; Grade II, $p = 0.035$; Grade III, $p = 0.085$; Grade IV, $p = 0.013$; Figure 11). Mean Grade I density on shady slopes (≈1830 stems ha^{-1}) was more than five times that on sunny slopes (≈340 stems ha^{-1}), a disparity likely reflecting the lower evapotranspiration demand and reduced photoinhibition stress on north-facing slopes in the subtropical monsoon environment, which are critical for the survival of *Cupressus funebris* seedlings during the prolonged dry season.

The synthesis of the analyses above the threshold with the environmental gradients identified by RDA and the variable importance rankings from PLS-SEM results in the following characterization of the optimal regeneration niche for *Cupressus funebris* in the study area: (1) shaded north-facing slopes; (2) canopy gap area exceeding approximately 10 m^2; (3) presence of soil rock fragments (Ssc > 0%), with regeneration density increasing weakly with higher rock fragment content; (4) moss coverage above 40%; (5) herb layer den-

sity below approximately 13,000 stems ha^{-1}; (6) tree density of 500–1500 stems ha^{-1} (not exceeding 2200); (7) elevations of 160–240 m; and (8) slope angles of 15–30°. The conditions under which these plants grow together are defined by the availability of light, the drainage of the substrate, the retention of moisture, and the level of interspecific competition. Together, these conditions define a regeneration niche that maximizes seedling establishment and survival in the subtropical monsoon environment of the Li River karst landscape.

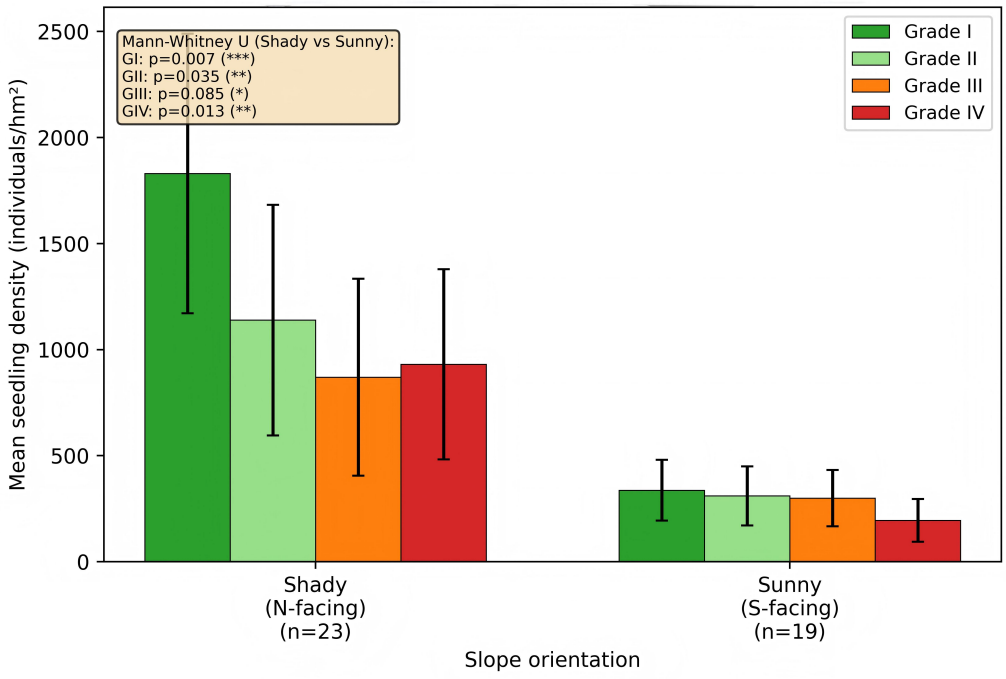


Figure 11. Slope orientation comparison. Note: *, **, and *** denote significance at $p \leq 0.1$, $p \leq 0.05$, and $p \leq 0.01$, respectively.

4. Discussion

4.1. Soil Stone Content as a Keystone Environmental Filter in Karst Regeneration

Among all environmental and stand structural variables examined, soil rock fragment content (Ssc) emerged as the single most influential predictor of *Cupressus funebris* regeneration, independently explaining 52.9% of the variation in the forward selection analysis and serving as the dominant indicator of the ENV construct in the PLS-SEM. This finding underscores the unique role of edaphic conditions in regulating plant regeneration in karst ecosystems, where soil development is inherently constrained by the underlying limestone geology [52].

Notably, the effect of Ssc on regeneration operated as a binary presence–absence mechanism rather than a continuous dose–response relationship. Segmented regression on the full dataset initially detected a significant breakpoint at Ssc ≈ 3.9%; however, supplementary analysis on the non-zero subset revealed no significant breakpoint, confirming that the apparent threshold was an artefact of the zero-inflated distribution of Ssc. Plots with any rock fragment content (Ssc > 0%) supported significantly higher regeneration density than rock-free plots across all seedling grades. This binary response can be attributed to multiple interacting mechanisms. Firstly, even a small proportion of rock fragments increases soil macroporosity and improves drainage, creating well-aerated rooting environments that favor the calciphilic root physiology of *Cupressus funebris* [53]. In karst landscapes, where shallow soils are susceptible to waterlogging during the monsoon season, enhanced drainage may be imperative for preventing root hypoxia in seedlings. Secondly, rock fragments function as thermal buffers, moderating diurnal soil temperature fluctuations

and maintaining a more stable microclimate for root growth [54]. Thirdly, the interstices between rock fragments provide physical microsites that protect newly germinated seedlings from surface runoff and soil erosion, processes that are particularly severe on karst slopes during heavy rainfall events characteristic of the Guilin region. The binary nature of this effect suggests that the critical ecological transition occurs at the onset of rock fragment presence, i.e., the shift from homogeneous fine-textured soil to a heterogeneous substrate containing even minimal rock fragments, rather than at any specific rock fragment proportion. This interpretation aligns with the concept of keystone substrate structures in karst pedology, whereby the initial introduction of coarse fragments significantly impacts soil hydrological and thermal regimes [55].

It should be noted that the binary effect does not imply that extremely high rock fragment content is equally favorable. Plots with Ssc $>$ 50% were rare in our dataset ($n = 1$), precluding robust statistical evaluation of the upper extreme. Nevertheless, the absence of a significant continuous trend within the Ssc > 0 subset suggests that, within the range observed in this study, the presence of rock fragments is more ecologically meaningful than their precise proportion. Future studies with larger sample sizes across a wider Ssc gradient would be needed to determine whether a decline in regeneration occurs at very high rock fragment content where soil volume becomes critically limiting.

The predominance of Ssc in explaining variations in regeneration, superseding other environmental variables such as altitude, slope, and rock exposure rate, is a salient observation. Although altitude and slope are widely accepted as the primary drivers of forest regeneration in mountainous regions [56,57], the relatively narrow elevation range (149–348 m) and low-relief karst peak-cluster landscape of the Li River Basin are likely to have served to attenuate the influence of these topographic gradients. In contrast, Ssc exhibited extreme spatial heterogeneity, reflecting the mosaic of soil development stages typical of karst terrain. This result indicates that in low-elevation karst landscapes, edaphic heterogeneity takes precedence over topographic gradients as the predominant environmental filter for tree regeneration. The finding contrasts markedly with regeneration patterns reported for non-karst montane forests, where altitude and slope are typically the dominant environmental filters [9,56]. In temperate forests of Hungary, for example, Tinya et al. [7] identified light availability and soil moisture as the primary regeneration drivers, with edaphic rock content playing a negligible role. Similarly, in the subtropical forests of the Loess Plateau, Wang et al. [6] found that microhabitat factors related to soil depth and litter accumulation, rather than rock fragment content, governed understory regeneration. The divergence observed in our study can be attributed to the fundamental geological distinction of karst landscapes: the carbonate bedrock undergoes differential dissolution, creating a mosaic of soil pockets with highly variable rock fragment content over spatial scales of meters [58]. This pedological heterogeneity, absent in non-karst systems, elevates Ssc from a secondary to a primary ecological filter. The karst-specific mechanism thus represents a departure from general regeneration theory and highlights the need for region-specific models when managing plantations on carbonate substrates. Whether this phenomenon extends to other karst plantation systems in subtropical China warrants further investigation.

4.2. Stand Structure as the Proximal Mediator of Environmental Effects on Regeneration

A key finding of this study is that environmental factors influence *Cupressus funebris* regeneration primarily through an indirect pathway mediated by stand structural attributes, rather than through direct effects on seedling establishment. The PLS-SEM revealed that the direct effect of ENV on REGEN was non-significant, whereas the indirect effect via STAND was substantial, accounting for 47.5% of the total effect. This mediation pattern

was further corroborated by the variation partitioning analysis, which showed that the shared fraction [ab] between environmental and stand structural variables far exceeded the pure environmental effect [a], indicating that most of the environmental influence on regeneration is channeled through its covariation with stand structure.

This finding is of significant theoretical importance. The majority of extant studies on *Cupressus funebris* regeneration have treated environmental and stand factors as independent, additive predictors [59]. The results obtained demonstrate that these two factor groups are causally linked in a hierarchical manner, with environmental factors operating as distal drivers and stand structure as the proximal mechanism. This hierarchical framework resolves the apparent incongruity observed in the extant literature, wherein both environmental and stand factors have been reported as primary drivers. These factors, it is posited, operate at different levels of the same causal chain.

The substantial shared variance component ([ab] = 41.2%) lends further credence to this interpretation. Rather than representing statistical redundancy, this shared fraction reflects the ecological reality that stand structure in karst plantations is fundamentally shaped by the underlying environmental template. Those in managerial roles who are keen to promote regeneration cannot simply manipulate stand structure without first considering the environmental constraints that determine the feasibility and sustainability of such interventions.

4.3. Gap Dynamics and Understory Facilitation

Canopy gap fraction emerged as the dominant stand structural driver of regeneration, ranking second only to Ssc in the forward selection and serving as the primary indicator of the STAND construct in the PLS-SEM. The strong positive correlation between gap area and regeneration across all ontogenetic grades confirms the critical role of gap dynamics in *Cupressus funebris* plantation succession.

Segmented regression identified a breakpoint at Gap $\approx$ 10.49 m^2 (95% CI: 6.42–14.57 m^2), below which regeneration density increased steeply with gap area (slope $\alpha_1 = 0.579$, $p < 0.001$) and above which the response plateaued (slope $\alpha_2 = 0.052$, $p = 0.079$). This breakpoint likely corresponds to the minimum light availability required for *Cupressus funebris* photosynthetic compensation, given that this species transitions from shade tolerance in the germination stage to increasing light demand as seedlings develop [60]. The existence of a discrete threshold, as opposed to a gradual response, suggests a non-linear relationship between light availability and seedling recruitment, consistent with gap-phase regeneration dynamics observed in other subtropical plantation systems [61]. Grouped comparison corroborated this pattern: mean total seedling density rose from 327 stems ha^{-1} in the 0–5 m^2 class to 7133 stems ha^{-1} in the >20 m^2 class (Kruskal–Wallis test, $p < 0.001$; Figure 9a), with the sharpest transition occurring between the 5–10 m^2 and 10–20 m^2 classes, consistent with the estimated breakpoint.

Within the understory, the opposing effects of moss coverage (facilitation) and herbaceous vegetation (competition) created a biotic interaction gradient that further modulated regeneration success. Moss coverage showed the strongest positive correlation with regeneration among all stand factors, and the threshold analysis identified 40% moss coverage as a critical facilitation threshold. The facilitative mechanism of moss operates through multiple pathways: moisture retention that buffers regeneration desiccation during dry periods, substrate stabilization that prevents seed displacement on karst slopes, and competitive suppression of herbaceous species through physical pre-emption of growing space [62]. This moss-mediated facilitation is particularly relevant in karst ecosystems, where thin soils and high drainage rates create chronic moisture stress for establishing seedlings.

Conversely, herbaceous density exceeding approximately 13,000 stems ha^{-1} triggered a sharp decline in Grade I seedling abundance, indicating competitive exclusion at the

earliest regeneration stage. The negative loading of HerbDen on the STAND construct indicates that herbaceous competition functions as a regeneration barrier within the stand structural pathway. This competitive threshold is of ecological significance as it marks the point at which the understory transitions from a facilitative (moss-dominated) to a competitive (herb-dominated) state. This transition has direct implications for the timing of management intervention.

The interplay between gap dynamics, understory interactions, and slope orientation can be synthesized that canopy gaps exceeding approximately 10 m^2 provide the necessary light resources for regeneration, but the realized regeneration outcome depends on both the biotic composition of the gap understory (facilitative moss vs. competitive herbs) and the mesotopographic context. Shady (north-facing) slopes supported Grade I seedling densities more than five times higher than sunny (south-facing) slopes, reflecting the lower evapotranspiration demand and reduced photoinhibition stress that characterize north-facing aspects in the subtropical monsoon environment. This slope orientation effect operated consistently across all developmental grades, indicating that aspect-mediated moisture availability is a persistent filter throughout the regeneration process, not merely a germination-stage constraint. The integration of gap dynamics, understory biotic interactions, and slope orientation is consistent with an expanded two-filter model of forest regeneration [63], in which abiotic conditions (light via gaps, moisture via aspect) and biotic interactions (moss facilitation vs. herb competition) act as sequential and interactive filters on seedling recruitment.

4.4. Ontogenetic Shifts in Regeneration Constraints

The empirical findings revealed a notable pattern, in which the strength of association between environmental factors and regeneration increased progressively from Grade I to Grade IV. This ontogenetic shift indicates that environmental filtering intensifies as seedlings develop, consistent with the ecological concept of increasing niche conservatism with plant age [63]. For seedlings classified as Grade I, the process of regeneration was predominantly influenced by stand structural factors, namely gap area and moss coverage. This finding underscores the significance of immediate microsite conditions for the successful germination and initial establishment of seeds. As saplings progress to Grade IV ($H \geq 100$ cm), environmental factors such as soil substrate quality and topographic position become increasingly important. This is likely because larger saplings have greater resource demands that can only be met under favorable macro-environmental conditions.

This ontogenetic pattern has a critical management implication: the bottleneck for *Cupressus funebris* regeneration is not seed germination (Grade I seedlings were abundant where regeneration occurred) but rather the survival and growth transition from early seedlings to established saplings (Grades III–IV). In order to overcome this bottleneck, it is necessary for favorable conditions to be sustained across both stand structural (adequate light, low competition) and environmental (suitable soil substrate, appropriate topographic position) dimensions.

4.5. Management Implications for Karst Cypress Plantation Restoration

Based on the quantitative thresholds identified in this study, a set of silvicultural guidelines can be proposed and ordered according to their relative importance in the causal pathway. The most critical intervention is selective thinning to maintain tree density within the optimal range of 500–1500 stems ha^{-1}, not exceeding the competitive exclusion threshold of 2200 stems ha^{-1}, while simultaneously creating canopy gaps exceeding approximately 10 m^2. LOWESS analysis revealed a hump-shaped response of Grade I seedling density to tree density, with peak regeneration at 500–1500 stems ha^{-1}

and near-complete suppression above 2200 stems ha^{-1}, providing site-specific benchmarks for thinning intensity in karst *Cupressus* plantations.

Retaining and promoting moss ground cover above 40% during and after management operations is equally important. This requires minimizing soil surface disturbance during thinning and avoiding practices that remove or damage the moss layer. As moss coverage showed the strongest positive correlation with regeneration among all stand factors, its facilitative role in seedling establishment makes it a cost-effective, nature-based approach to regeneration promotion that should be integrated into standard operational protocols.

Additionally, targeted control of herbaceous vegetation is recommended when density exceeds 13,000 stems ha^{-1}, particularly in recently created canopy gaps, where rapid herb colonization may outpace seedling establishment. Selective weeding is preferable to broadcast herbicide application in order to preserve the moss layer and maintain the facilitative understory conditions identified above.

At the landscape planning level, regeneration management efforts should prioritize shady (north-facing) slopes with a presence of soil rock fragments (Ssc $>$ 0%), as shady slopes supported five times higher seedling densities than sunny slopes, and even minimal rock fragment content can significantly improve substrate conditions for regeneration. On south-facing slopes or rock-free soils, where these natural facilitative conditions are absent, supplementary measures such as artificial shading or surface mulching with coarse substrate may be necessary to achieve comparable regeneration outcomes.

Taken together, these recommendations follow a hierarchical logic that is consistent with the mediation pathway (ENV $\rightarrow$ STAND $\rightarrow$ REGEN) identified by the PLS-SEM. Thinning and gap creation modify the proximal stand structural drivers; moss retention and herb control optimize the biotic understory environment; and site selection leverages the distal environmental template that underpins the entire causal chain.

5. Conclusions and Future Perspectives

5.1. Conclusions

This study provides an improved understanding of the environmental and stand structural factors influencing natural regeneration of *Cupressus funebris* plantations in the karst landscape of the Li River Basin, southern China. Using redundancy analysis, variation partitioning, and partial least squares structural equation modeling across 54 sample plots, we identified soil rock fragment content and canopy gap area as the most critical predictors, collectively explaining the majority of regeneration variation. Variation partitioning revealed that the shared component between environmental and stand structural factors dominated over pure effects, and PLS-SEM further demonstrated that environmental factors influence regeneration primarily through an indirect pathway mediated by stand structure, explaining 68.3% of regeneration variance. Threshold analysis identified quantitative benchmarks for key drivers: presence of soil rock fragments, canopy gap area exceeding approximately 10 m^2, moss coverage $>$40%, herb density $<$13,000 stems ha^{-1}, tree density of 500–1500 stems ha^{-1} (not exceeding the competitive exclusion threshold of 2200 stems ha^{-1}), and shady (north-facing) slope orientation. These findings support a close-to-nature silvicultural approach where selective thinning, moss layer retention, herbaceous competition control, and prioritization of north-facing slopes with rock-bearing substrates can effectively promote natural regeneration by optimizing the proximal stand structural conditions identified in the mediation pathway.

5.2. Limitations and Future Directions

Despite the comprehensive insights derived from this study, there are several intrinsic limitations that must be critically acknowledged. First, the cross-sectional design

precludes strict causal inference; the mediation pathway identified by PLS-SEM requires validation through experimental manipulation or longitudinal monitoring. Second, the sample size ($n = 54$) constrained model complexity, preventing the inclusion of factors such as seed source availability, herbivory pressure, and anthropogenic disturbance that likely contributed to unexplained variance. Although segmented regression was applied to the two dominant predictors (Gap and Ssc), thresholds for other variables were derived from grouped comparisons and LOWESS smoothing rather than formal breakpoint testing; future work should apply segmented regression or CART to these variables with larger samples. Third, the analysis was confined to the stand scale, leaving landscape-level drivers unexamined. Given the sensitivity of karst ecosystems to hydrological perturbations, future research should evaluate the resilience of *Cupressus funebris* regeneration under projected climate change scenarios, particularly shifts in precipitation regimes and thermal conditions [57]. Fourth, the plots were distributed across eight sub-areas spanning approximately 40 km along the Li River, introducing potential spatial autocorrelation that was not explicitly modeled [64]. The bootstrapping procedure in PLS-SEM yields standard errors robust to non-normality [42]; however, it assumes exchangeable observations and therefore cannot account for inflated Type I error rates associated with spatial dependence. Future studies could incorporate spatially explicit models or mixed-effects models with site as a random effect to formally address this structure. More broadly, integrating remote sensing for landscape-scale monitoring, microclimatic sensors for fine-scale environmental characterization, and molecular ecology for genetic diversity assessment would substantially advance understanding of regeneration dynamics in karst cypress forests.

Author Contributions: Conceptualization, Y.G. and W.L.; methodology, Y.G.; software, Y.G. and D.L.; validation, Y.G., Y.H. and H.Y.; formal analysis, Y.G.; investigation, Y.G., D.L. and Y.H.; resources, W.L.; data curation, Y.G. and D.L.; writing—original draft preparation, Y.G.; writing—review and editing, Y.G. and W.L.; visualization, Y.H. and H.Y.; supervision, W.L.; project administration, W.L.; funding acquisition, W.L. and Y.G. All authors have read and agreed to the published version of the manuscript.

Funding: This research was funded by the Key Laboratory of Karst Ecosystem and Treatment of Rocky Desertification, Ministry of Natural Resources, Institute of Karst Geology, CAGS, under the project "Research on the Interaction Mechanism between Rural Revitalization Industry and the Effectiveness of Rocky Desertification Management in Karst Region", grant number BL202106; Supported by the Guangxi Key Science and Technology Innovation Base on Karst Dynamics; and the Office of Philosophy and Social Sciences of the Guangxi Zhuang Autonomous Region under the 2025 Annual Research Project in Philosophy and Social Sciences of Guangxi, titled "Cross-Border Coordination Mechanisms for Realizing the Value of Guangxi-ASEAN Ecological Products under the RCEP Framework", grant number 25JYF173.

Institutional Review Board Statement: Not applicable.

Informed Consent Statement: Not applicable.

Data Availability Statement: The data presented in this study are contained within the article.

Acknowledgments: The authors express their gratitude to the Institute of Karst Geology, CAGS for providing the experimental platform. During the preparation of this manuscript, the authors used generative AI tools for linguistic polishing and formatting assistance. The authors have reviewed and edited the output and take full responsibility for the content of this publication.

Conflicts of Interest: Author Dingyuan Liu was employed by the company Shandong Lan'an Landscape Engineering Co., Ltd. The remaining authors declare that the research was conducted in the absence of any commercial or financial relationships that could be construed as a potential conflict of interest.

Abbreviations

The following abbreviations are used in this manuscript:

Al	Altitude
CC	Canopy Closure
CypDen	*Cupressus funebris* Density
DBH	Diameter at Breast Height
ENV	Environmental Factors (Latent Construct)
Gap	Canopy Gap Area
GLD	Ground-line Diameter
HerbCov	Herb Coverage
HerbDen	Herb Density
LOWESS	Locally Weighted Scatterplot Smoothing
MossCov	Moss Coverage
PLS-SEM	Partial Least Squares Structural Equation Modeling
R	Rock Exposure Rate
RDA	Redundancy Analysis
REGEN	Regeneration (Latent Construct)
S	Slope
SRMR	Standardized Root Mean Square Residual
Ssc	Soil Rock Fragment Content
STAND	Stand Structure (Latent Construct)
ShrubCov	Shrub Coverage
ShrubDen	Shrub Density
TreeDen	Tree Density
VIF	Variance Inflation Factor

Appendix A

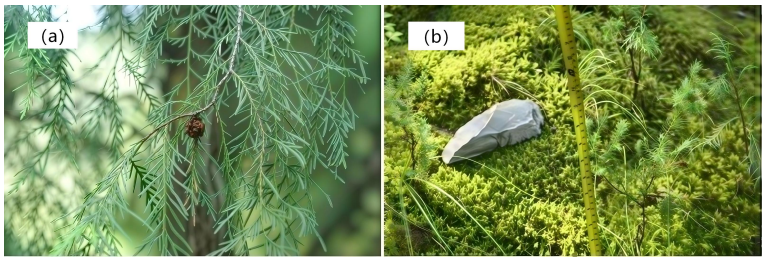


Figure A1. Photographs of *Cupressus funebris* in the Li River karst landscape: (**a**) mature tree branch bearing ripe cones; (**b**) naturally regenerated seedlings establishing on a moss-covered rocky substrate. (Photos taken during field surveys, 2020–2023.)

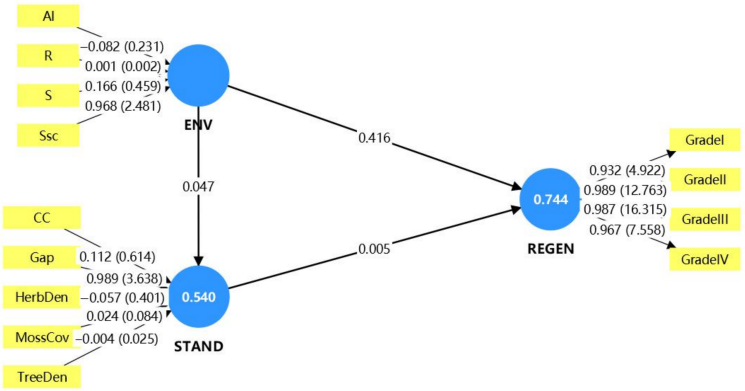


Figure A2. PLS-SEM: Effects of environmental factors and stand structure on the regeneration of *Cupressus funebris* in karst landscapes of the Li River basin ($n = 36$).

Table A1. Conditional effects of individual variables on *Cupressus* regeneration tested by permutational ANOVA (Type III).

Variable	Category	Conditional R^2	*p*-Value
R	Environmental	0.040	0.038
MossCov	Stand structure	0.039	0.038
TreeDen	Stand structure	0.026	0.140
HerbCov	Stand structure	0.023	0.163
Al	Environmental	0.016	0.276
Gap	Stand structure	0.017	0.287
CypDen	Stand structure	0.012	0.408
ShrubDen	Stand structure	0.011	0.440
CC	Stand structure	0.010	0.476
S	Environmental	0.011	0.495
HerbDen	Stand structure	0.010	0.525
Ssc	Environmental	0.007	0.589
ShrubCov	Stand structure	0.007	0.686

Note: Conditional R^2 represents the unique variance explained by each variable after accounting for all other variables in the full model. Significance was assessed using 999 permutations. Variables are ordered by *p*-value.

Table A2. Variance inflation factors (VIFs) for all indicators in the PLS-SEM model.

Construct	Indicator	VIF
ENV	Al	1.344
	R	1.261
	S	1.467
	Ssc	1.098
STAND	CC	1.350
	Gap	2.357
	HerbDen	1.179
	MossCov	2.333
	TreeDen	1.322

Table A3. Measurement model weights of PLS-SEM.

Construct	Indicator	Outer Weight	*t*-Value
ENV	Al	−0.019	0.085
	R	0.031	0.225
	S	0.178	0.786
	Ssc	0.963	4.711
STAND	CC	0.096	0.622
	Gap	1.091	3.586
	HerbDen	−0.063	0.492
	MossCov	−0.111	0.337
	TreeDen	0.061	0.563

Table A4. Sensitivity analysis of full model and reduced model.

Path	Full Model ($n = 54$) β	Full Model *p*-Value	Reduced Model ($n = 36$) β	Reduced Model *p*-Value
ENV → STAND	0.711	<0.001	0.735	0.047
ENV → REGEN	0.394	0.240	0.259	0.416
STAND → REGEN	0.499	0.067	0.654	0.005
ENV → STAND → REGEN (indirect)	0.355	0.073	0.481	0.100

References

1. Vieira, D.L.; Scariot, A. Principles of natural regeneration of tropical dry forests for restoration. *Restor. Ecol.* **2006**, *14*, 11–20. [CrossRef]
2. Cheng, R.; Shen, Y.; Feng, X.; Xiao, W.; Wang, N.; Yang, S.; Guo, Y. Research review on forests natural regeneration. *J. Zhejiang A & F Univ.* **2018**, *35*, 955–967.
3. Chazdon, R.L.; Guariguata, M.R. Natural regeneration as a tool for large-scale forest restoration in the tropics: Prospects and challenges. *Biotropica* **2016**, *48*, 716–730. [CrossRef]

4. Lewis, S.L.; Edwards, D.P.; Galbraith, D. Increasing human dominance of tropical forests. *Science* **2015**, *349*, 827–832. [CrossRef]
5. Yang, Z.; Wu, Y.; Chen, S.; Sui, M.; Zhang, G.; Liu, Q.; Chen, D.; He, Y.; Zang, L. Does the universal adaptive strategy theory apply to natural regeneration in heterogeneous subtropical karst forests. *Ecol. Indic.* **2024**, *165*, 112168. [CrossRef]
6. Wang, Z.; Jiang, L.; Gao, J.; Qing, S.; Pan, C.; Wu, Y.; Yang, H.; Wang, D. The influence of microhabitat factors on the regeneration and species composition of understory woody plants in *Pinus tabuliformis* plantations on the Loess Plateau. *For. Ecol. Manag.* **2022**, *509*, 120080. [CrossRef]
7. Tinya, F.; Márialigeti, S.; Bidló, A.; Ódor, P. Environmental drivers of the forest regeneration in temperate mixed forests. *For. Ecol. Manag.* **2019**, *433*, 720–728. [CrossRef]
8. Lu, Y.L.; Zhang, W.H.; Yang, B.; Wang, Y.N. Seed rain, soil seed bank and seedling regeneration of *Quercus aliena* var. *acuteserrata* in different slope directions on the middle Qinling Mountains, China. *J. Appl. Ecol.* **2019**, *30*, 1965–1973.
9. Redmond, M.D.; Kelsey, K.C. Topography and overstory mortality interact to control tree regeneration in spruce-fir forests of the southern Rocky Mountains. *For. Ecol. Manag.* **2018**, *427*, 106–113. [CrossRef]
10. Zhang, Y.; Wei, X.; Liang, W.J.; Liu, Z.Q.; Li, F.M.; Zhao, Y.; Feng, Y.H. Effects of Gap Size on Regeneration Dynamics of *Larix principis-rupprechtii* Forest. *For. Res.* **2022**, *35*, 84–92.
11. Wang, W.R.; Liu, S.; Tian, J.X.; Hou, Z.Y.; Zhao, S.B. Effect of Canopy Density on Regeneration Growth of Young Trees under *Larix olgensis* Plantation. *J. Beihua Univ. Nat. Sci.* **2020**, *21*, 724–729.
12. Huong, P.V.; Chen, C.X.; Zhang, Q.Q.; Tung, H.V. The Effect of Shrub and Herb on the Population Regeneration and Density of *Sterculia lychnophora* Saplings and Seedling. *J. Southwest For. Univ. Nat. Sci.* **2016**, *36*, 1–8.
13. Schweier, J.; Blagojević, B.; Venanzi, R.; Latterini, F.; Picchio, R. Sustainability assessment of alternative strip clear cutting operations for wood chip production in renaturalization management of pine stands. *Energies* **2019**, *12*, 3306. [CrossRef]
14. Dyderski, M.K.; Jagodziński, A.M. Drivers of invasive tree and shrub natural regeneration in temperate forests. *Biol. Invasions* **2018**, *20*, 2363–2379. [CrossRef]
15. Kuuluvainen, T.; Gauthier, S. Young and old forest in the boreal: Critical stages of ecosystem dynamics and management under global change. *For. Ecosyst.* **2018**, *5*, 1–15. [CrossRef]
16. Song, T.Q.; Peng, W.X.; Zeng, F.P.; Wang, K.L.; Ouyang, Z.W. Vegetation succession rule and regeneration strategies in disturbed karst area, northwest Guangxi. *J. Mt. Sci.* **2008**, *26*, 597–604.
17. Li, R.; Gao, J.; He, M.; Jing, J.; Xiong, L.; Chen, M.; Zhao, L. Effect of rock exposure on runoff and sediment on karst slopes under erosive rainfall conditions. *J. Hydrol. Reg. Stud.* **2023**, *50*, 101525. [CrossRef]
18. Yang, J.; Huang, Y.; Su, M.; Liu, M.; Yang, J.; Wu, Q. Spatial distribution patterns of the key afforestation species *Cupressus funebris*: Insights from an ensemble model under climate change scenarios. *Forests* **2024**, *15*, 1280. [CrossRef]
19. Xie, C.; Li, M.; Jim, C.Y.; Liu, D. Environmental factors driving the spatial distribution pattern of venerable trees in Sichuan Province, China. *Plants* **2022**, *11*, 3581. [CrossRef]
20. Farahmand, H. The genus *Cupressus* L. mythology to biotechnology with emphasis on mediterranean cypress (*Cupressus sempervirens* L.). *Hortic. Rev.* **2020**, *47*, 213–287.
21. Weiss, R. *Trees of the Rocky Mountains: Identifying the Region's Prominent Trees*; Rowman & Littlefield: Lanham, MD, USA, 2025.
22. Quintero, C.J.; Cohen, M.J. Scale-dependent patterning of wetland depressions in a low-relief karst landscape. *J. Geophys. Res. Earth Surf.* **2019**, *124*, 2101–2117. [CrossRef]
23. Kimambo, N.E.; Naughton-Treves, L. The role of woodlots in forest regeneration outside protected areas: Lessons from Tanzania. *Forests* **2019**, *10*, 621. [CrossRef]
24. Slye, J.N.; Lang, A.J.; Gerow, T.A., Jr. A limited rapid assessment of forest regeneration in 24 cypress and tupelo bottomland swamps following clearcutting and shovel logging in the coastal plain of North Carolina. *Forests* **2020**, *11*, 854. [CrossRef]
25. Conner, W.H.; Toliver, J.R.; Sklar, F.H. Natural regeneration of baldcypress (*Taxodium distichum* (L.) Rich.) in a Louisiana swamp. *For. Ecol. Manag.* **1986**, *14*, 305–317. [CrossRef]
26. Qin, P.; Huang, Y.; Zheng, W.J.; Yu, H.; Zhang, Q.; Xie, Z.; Gao, Y.; Bu, Y.; Gan, Y. Factors affecting natural regeneration of *Platycladus orientalis* (L.) Franco in Guilin, China. *Sumar. List.* **2022**, *146*, 403–414. [CrossRef]
27. Guangxi Bureau of Statistics. *Guangxi Statistical Yearbook 2023*; China Statistics Press: Beijing, China, 2023.
28. Guangxi Bureau of Statistics. Guangxi Statistical Database. 2023. Available online: http://tjj.gxzf.gov.cn/ (accessed on 15 October 2023).
29. Xu, Z.B.; Dai, L.M.; Chen, J.Q.; Wang, Z.; Dai, H.; Cai, L.X. Natural regeneration condition in *Pinus koraiensis* broad-leaved mixed forest. *Acta Ecol. Sin.* **2001**, *21*, 1413–1420.
30. von Lüpke, B. Silvicultural methods of oak regeneration with special respect to shade tolerant mixed species. *For. Ecol. Manag.* **1998**, *106*, 19–26. [CrossRef]
31. Liu, D.Q.; Cao, E.J.; Zhang, J.X.; Gong, J.; Yan, L.L. Spatiotemporal pattern of water conservation and its influencing factors in Bailongjiang Watershed of Gansu. *J. Nat. Resour.* **2020**, *35*, 1728–1743. [CrossRef]
32. Xie, Y.G.; Li, X. Methodology on rock fragments content evaluation: A review. *Soils* **2012**, *44*, 17–22.

33. Lin, W.; Meng, Y.; Qiu, Z.; Zhang, S.; Wu, J. Measurement and calculation of crown projection area and crown volume of individual trees based on 3D laser-scanned point-cloud data. *Int. J. Remote Sens.* **2017**, *38*, 1083–1100. [CrossRef]
34. Li, Y.N.; Zhang, B.L.; Qin, S.Y.; Li, S.Y.; Huang, X.R. Review of research and application of forest canopy closure and its measuring methods. *World For. Res.* **2008**, *21*, 40.
35. Keyghobadi, M.; Sahragard, H.P.; Rad, M.R.P.; Karami, P.; Yari, R. Application of generalized additive model and classification and regression tree to estimate potential habitat distribution of range plant species (case study: Khazri rangelands of Beyaz Plain, southern Khorasan). *Iran. J. Range Desert Res.* **2020**, *27*, 561–576.
36. Jamali, H.; Ghehsareh Ardestani, E.; Ebrahimi, A.; Pordel, F. Comparing distance-based methods of measuring plant density in an arid sparse scrubland: Testing field and simulated sampling. *Environ. Monit. Assess.* **2020**, *192*, 343. [CrossRef]
37. Li, H.; Zhang, X.; Li, Z.; Wen, J.; Tan, X. A review of research on tree risk assessment methods. *Forests* **2022**, *13*, 1556. [CrossRef]
38. Floyd, D.A.; Anderson, J.E. A comparison of three methods for estimating plant cover. *J. Ecol.* **1987**, *75*, 221–228. [CrossRef]
39. Sarstedt, M.; Richter, N.F.; Hauff, S.; Ringle, C.M. Combined importance–performance map analysis (cIPMA) in partial least squares structural equation modeling (PLS–SEM): A SmartPLS 4 tutorial. *J. Mark. Anal.* **2024**, *12*, 746–760. [CrossRef]
40. Legendre, P.; Gallagher, E.D. Ecologically meaningful transformations for ordination of species data. *Oecologia* **2001**, *129*, 271–280. [CrossRef]
41. Borcard, D.; Legendre, P.; Drapeau, P. Partialling out the spatial component of ecological variation. *Ecology* **1992**, *73*, 1045–1055. [CrossRef]
42. Hair, J.F.; Risher, J.J.; Sarstedt, M.; Ringle, C.M. When to use and how to report the results of PLS-SEM. *Eur. Bus. Rev.* **2019**, *31*, 2–24. [CrossRef]
43. Diamantopoulos, A.; Sarstedt, M.; Fuchs, C.; Wilczynski, P.; Kaiser, S. Guidelines for choosing between multi-item and single-item scales for construct measurement: A predictive validity perspective. *J. Acad. Mark. Sci.* **2012**, *40*, 434–449. [CrossRef]
44. Wagner, R.; Grimm, M.S. Empirical validation of the 10-times rule for SEM. In *State of the Art in Partial Least Squares Structural Equation Modeling (PLS-SEM) Methodological Extensions and Applications in the Social Sciences and Beyond*; Springer: Kassel, Germany, 2023; pp. 3–7.
45. Hair, J.F., Jr.; Matthews, L.M.; Matthews, R.L.; Sarstedt, M. PLS-SEM or CB-SEM: Updated guidelines on which method to use. *Int. J. Multivar. Data Anal.* **2017**, *1*, 107–123. [CrossRef]
46. Muggeo, V.M.R. Estimating regression models with unknown break-points. *Stat. Med.* **2003**, *22*, 3055–3071. [CrossRef]
47. Pilgrim, C. piecewise-regression (aka segmented regression) in Python. *J. Open Source Softw.* **2021**, *6*, 3859. [CrossRef]
48. Fisher, N.I.; Lewis, T.; Embleton, B.J.J. *Statistical Analysis of Spherical Data*; Cambridge University Press: Cambridge, UK, 1993.
49. Blanchet, F.G.; Legendre, P.; Borcard, D. Forward selection of explanatory variables. *Ecology* **2008**, *89*, 2623–2632. [CrossRef]
50. Henseler, J.; Hubona, G.; Ray, P.A. Using PLS path modeling in new technology research: Updated guidelines. *Ind. Manag. Data Syst.* **2016**, *116*, 2–20. [CrossRef]
51. Zhao, X.; Lynch, J.G., Jr.; Chen, Q. Reconsidering Baron and Kenny: Myths and truths about mediation analysis. *J. Consum. Res.* **2010**, *37*, 197–206. [CrossRef]
52. Liu, H.; Jiang, Z.; Dai, J.; Wu, X.; Peng, J.; Wang, H.; Meersmans, J.; Green, S.M.; Quine, T.A. Rock crevices determine woody and herbaceous plant cover in the karst critical zone. *Sci. China Earth Sci.* **2019**, *62*, 1756–1763. [CrossRef]
53. Yuan, C.Z.; Chen, T.; Zhang, Z.; Jin, G.Q.; Feng, Z.P.; Zhou, Z.C.; Zheng, Y. Effects of calcium addition on growth and root development of *Cupressus funebris* families in different nutrient conditions. *Chin. J. Appl. Environ. Biol.* **2020**, *26*, 1161–1168.
54. Zhang, Y.; Zhang, M.; Niu, J.; Li, H.; Xiao, R.; Zheng, H.; Bech, J. Rock fragments and soil hydrological processes: Significance and progress. *Catena* **2016**, *147*, 153–166. [CrossRef]
55. Hlaváčiková, H.; Novák, V.; Kostka, Z.; Danko, M.; Hlavčo, J. The influence of stony soil properties on water dynamics modeled by the HYDRUS model. *J. Hydrol. Hydromech.* **2018**, *66*, 181. [CrossRef]
56. Márialigeti, S.; Tinya, F.; Bidló, A.; Ódor, P. Environmental drivers of the composition and diversity of the herb layer in mixed temperate forests in Hungary. *Plant Ecol.* **2016**, *217*, 549–563. [CrossRef]
57. Trang, P.T.; Thu, N.T.; Son, L.T.; Dung, T.V.; An, T.T.; Thuong, P.T.; Quy, N.V.; Nhung, T.T.; Baniya, C.B.; Dagamac, N.H.; et al. Impacts of climate change on the distribution of Vietnamese golden cypress in Northern Vietnam. *Biol. Bull. Rev.* **2024**, *14*, 505–518. [CrossRef]
58. Ford, D.; Williams, P.D. *Karst Hydrogeology and Geomorphology*; John Wiley & Sons: Hoboken, NJ, USA, 2007.
59. Chen, J.; Mou, H.; Xie, T.; Bie, P.; Mu, C. Hydrological Effects of Litter Layer and Soil Layer in *Cupressus funebris* Plantation under Different Thinning Intensities in Hilly Area of Central Sichuan. *J. Sichuan For. Sci. Technol.* **2020**, *41*, 8–14.
60. Li, X.Y.; Pan, P.; Zang, H.; Ning, J.; Ouyang, X.; Li, X.; Lin, Y.; Wu, Z. Study on factors affecting natural regeneration of natural secondary *Phoebe bournei* forest. *For. Res.* **2017**, *30*, 701–708.
61. Yang, Y.L.; Li, X.W.; Zhou, Y.G.; Li, Y.K. Effects of gap thinning on growth and diversity of a cypress plantation in the hilly region of central Sichuan. *Chin. J. Appl. Environ. Biol.* **2014**, *19*, 922–928.

62. Soudzilovskaia, N.A.; Graae, B.J.; Douma, J.C.; Grau, O.; Milbau, A.; Shevtsova, A.; Wolters, L.; Cornelissen, J.H. How do bryophytes govern generative recruitment of vascular plants? *New Phytol.* **2011**, *190*, 1019–1031. [CrossRef] [PubMed]
63. Grubb, P.J. The maintenance of species-richness in plant communities: The importance of the regeneration niche. *Biol. Rev.* **1977**, *52*, 107–145. [CrossRef]
64. Dormann, C.F.; McPherson, J.M.; Araújo, M.B.; Bivand, R.; Bolliger, J.; Carl, G.; Davies, R.; Hirzel, A.; Jetz, W.; Kissling, W.D.; et al. Methods to account for spatial autocorrelation in the analysis of species distributional data: A review. *Ecography* **2007**, *30*, 609–628. [CrossRef]

Disclaimer/Publisher's Note: The statements, opinions and data contained in all publications are solely those of the individual author(s) and contributor(s) and not of MDPI and/or the editor(s). MDPI and/or the editor(s) disclaim responsibility for any injury to people or property resulting from any ideas, methods, instructions or products referred to in the content.